DEGREE PROJECT

# Trajectory Optimization of Round Trip to Arjuna-type Near-Earth Asteroids from a Lunar Distant Retrograde Orbit Using Lunar Gravity Assist

*Master's Degree in Spacecraft Design*

Muhammad Ansyar Rafi Putra

**Space Engineering, master's level (120 credits)**
**2019**

Luleå University of Technology
Department of Computer Science, Electrical and Space Engineering

LULEÅ UNIVERSITY OF TECHNOLOGY

*This page intentionally left blank*

**Abstract**

Asteroid mining is rapidly becoming a popular topic amongst space community, primarily due to the potential resources that the asteroids can provide for future spacefaring. One of the interesting resources that can be obtained from asteroids is water, which can also be processed into oxygen and fuel. An intriguing concept would be to process fuel from asteroid, and establish a fuel depot in an Earth-centered orbit. This thesis considers a mission concept consisting of travelling to an Arjuna near-Earth asteroid from a lunar distant retrograde orbit as a depot orbit, processing fuel in-situ from the water on the asteroid, and bringing back 100 tons of fuel to the depot orbit.

In order to minimize fuel consumption for such a trip, the thesis develops an optimization method that can obtain the best trajectory for different phases of the round trip, given certain constraints to ensure the spacecraft successfully reaches the asteroid and comes back to the Earth system.

The optimization model consists of four steps, i.e., the outbound trip, the first phase of the return trip, the second phase of the return trip, and the optimization for the combined phases of return trip. The outbound trip is the trajectory from the depot orbit to the asteroid. After at least three months of mining, the spacecraft brings back the processed fuel to the vicinity of the Moon. This phase is called the first phase of the return trip. The spacecraft is then captured without an insertion burn to an Earth-centered orbit by a lunar gravity assist maneuver, and travels to the point where the insertion maneuver to the depot orbit begins. This is the second phase of the return trip. The last step of the optimization is the combination of the two phases of return trip, in addition to the final maneuver for entering the lunar distant retrograde orbit.

The optimization method uses MATLAB *fmincon* solver, and it was applied to 29 synthetic asteroids. There were 19 converged solutions, but for 10 asteroids the optimizations was not able to converge. The lowest minimum fuel consumption for a trip is 19 965.5 kg, and the highest minimum fuel consumption is 61 821.4 kg. For the lowest minimum fuel consumption, the duration of the trip is nearly 7 years, and the duration for the highest minimum fuel consumption is about 2.6 years.

# Acknowledgements

I would like to thank my supervisor Prof. Reza Emami for the discussion, feedback, and suggestion during the development of the thesis.

I also want to thank my friends from all over the world for their encouragement during the process of the thesis.

Finally, I would like to thank my parents for their endless love and support, although they are in the other side of the world.

# Contents

# List of Figures

# List of Tables

# Abbreviations

| | |
|---|---|
| CRTBP | Circular Restricted Three-Body Problem |
| DRO | Distant Retrograde Orbit |
| GMAT | General Mission Analysis Tools |
| JAXA | Japan Aerospace Exploration Agency |
| LDRO | Lunar Distant Retrograde Orbit |
| LGA | Lunar Gravity Assist |
| NASA | National Aeronautics and Space Administration |
| NEA | Near-Earth Asteroids |

# Chapter 1

# Introduction

The thesis is focused on the design of a mission model and its fuel consumption optimization. The mission revolves around a round trip to an asteroid to mine its resources. The report is constructed from the following chapters.

Chapter 1: an introduction to the thesis motivation, purpose, and boundaries.

Chapter 2: a description of the theories used in the project.

Chapter 3: an explanation of how the model and optimization is constructed

Chapter 4: a compilation of results from the optimization

Chapter 5: a discussion and analysis of the results in Chapter 4.

Chapter 6: the summary of important discovery from the results.

## 1.1 Asteroids and Their Influence on Humanity

For decades, asteroids have started to attract attention and interest space community. One reason is to protect planet Earth from potential asteroids impact. A recent asteroid impact on Earth occurred in 2013, in Chelyabinsk, where an explosion was observed 27 km above the ground. The explosion caused an airburst that damaged properties and caused around 1600 injured citizens [1]. Different technologies for preventing hazardous impact are developed, from a laser technology [2] for detecting and characterizing the

asteroids, to crashing a spacecraft [3] into the asteroids in order to change their orbit.

Another reason is an effort to reveal the origin of the Solar System. Asteroids, as one of the closest neighbors of Earth, contain information for such purpose. They have been examined by the scientist, though, there is no direct contact on asteroids by humankind yet. Such an experiment would need the target object to be reachable by humankind. However, the farthest humankind has traveled in space was to the Moon in the Apollo program by NASA [4]. Considering the fact, it is improbable that humankind would travel to the asteroids in the near future. The second option is to bring the asteroid itself to the accessible orbit for astronauts. NASA developed an asteroid redirect mission [5], which will bring the asteroid into an Earth-centered orbit. The spacecraft would capture the asteroids with a giant robotic arm, then move it to Earth vicinity. The mission design was ended by White House Space Policy Directive 1, however, the technology is still being developed for future human spaceflight [6].

The last point of interest is the potential that the asteroids have. It has been known for years asteroids have an abundance of resources. Asteroids had been classified in [7] into several categories, such as C-type (carbon, hydrated minerals, and organic chemicals), S-type (metal and high levels of distinguishable minerals), and M-type (mostly metals). Because the resources on Earth is non-renewable, asteroid mining might become a profitable industry in the future. The realization of asteroid mining, however, has not been feasible because of the lack of necessary technologies. The spacecraft needs a good anchor to generate sufficient force to drill or cut the asteroid due to the zero-gravity effect. The possible mining method is explained further in [8]. One company called Trans Astronautica Corporation has started developing an optical mining technology focusing on water extraction, which is capable of mining asteroids at rates of up to tons per month [9]. An alternative mining concept with multiple small spacecraft, in which 100 kg of resources would be brought back to Earth, is also studied in [10].

## 1.2 Asteroids as Fuel Resources

The water contained in asteroids can also be processed into spacecraft fuel. This concept can be extended by adding a fuel depot in space and the asteroids as the source. The fuel depot in space would be the breakthrough to decrease launch cost as well as space travel to deep space. Planet Resources has proposed this idea and has started to prospect the feasible asteroids [11,12]. Conte et al [13], also discuss how Lunar Distant Retrograde Orbit (LDRO)

can be used for Earth-Mars transfer assuming a fuel depot is present in the LDRO.

The process of mining itself is not simple either. First, the feasible asteroids needs to be identified, then a spacecraft shall be sent to drill and store the resources. Assuming the mining technology capable of extracting and storing 100 000 kg of resources, bringing such weight to the Earth system has never been done before. The recent missions to asteroids are OSIRIS-REx by NASA [14] and Hayabusa 2 by JAXA [15]. Both spacecraft missions are to rendezvous with an asteroid and bring samples back to Earth for analysis. Furthermore, the predecessor of Hayabusa 2, Hayabusa [16], has successfully observed a near-Earth asteroid 25143 Itokawa and brought back a small amount of asteroid sample. The closest mission design is the NASA asteroid redirect robotic arm mission. They planned to bring an asteroid, with an estimated mass of 1 000 000 kg, with low-thrust electric propulsion [17]. The possible target asteroids are synthetic Arjuna-type Near-Earth Asteroids(NEA), which are close and have low inclination. The orbital transfer from Arjuna-type NEA using low thrust transfer is analyzed in [18].

One of the major challenges for asteroid fuel mining is how to make an efficient trip from the fuel depot to an asteroid and bring the fuel back to the Earth system. This thesis focuses on making an optimization routine which can determine the efficient trajectory assuming the fuel depot is in LDRO. A Lunar Gravity Assist (LGA) is also utilized to capture the spacecraft to the Earth system.

## 1.3 Purpose of the Thesis

The primary purposes of the thesis are shown below:

1. Design a simulation model that can perform a round trip mission from an LDRO to an asteroid using LGA to capture the spacecraft to the Earth system.

2. Utilize MATLAB *fmincon* optimizer to find an efficient trip for such a mission in term of fuel consumption.

3. Apply the optimization to various target asteroids.

The secondary objective is to find suitable parameters of the asteroids orbital elements that could act as the first filter when choosing the target asteroids.

## 1.4 Boundaries and Assumptions

The thesis project was done within several boundaries and assumptions.

1. The solar wind pressure is neglected.
2. The mining process is only defined by the mining duration.
3. The spacecraft is capable of mining 100 000 kg of fuel in 92 days.
4. The rendezvous process with the asteroid is considered to happen instantly.
5. The first converged result of the optimization shall be taken as the optimized result.

# Chapter 2

# Theory

To design the simulation model, some theories must be described. This chapter talks about the important theories for building the model.

## 2.1 Lunar Distant Retrograde Orbit (LDRO)

Distance Retrograde Orbit(DRO) is an unconventional orbit that is the results of Circular Restricted Three-Body Problem (CRTBP) [19]. The spacecraft in DRO is affected by two astronomical objects. In the case of Lunar DRO, Earth is the primary body and Moon is the secondary body. Figure 2.1 shows one example of LDRO.

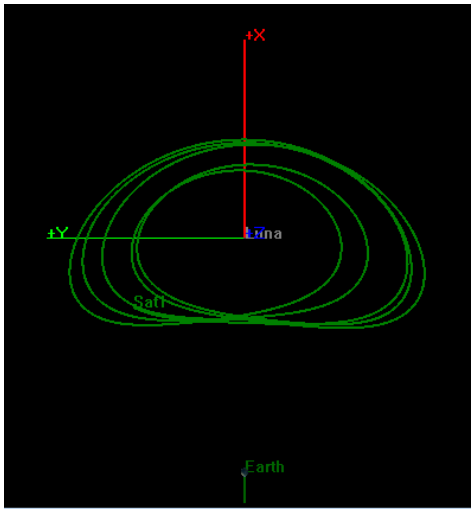


Figure 2.1: Lunar Distant Retrograde Orbit with 125 000 km distance from the center of the Moon.

In Figure 2.1, it can be seen that the shape of the orbit is unusual. The shape looks almost like an ellipse, except, there is a part on the left and right side of the picture, where the orbit gets pulled by Earth gravity. Another interesting remark, the orbital elements of the spacecraft in such orbit always change over time. At the beginning of the simulation of the orbit in Figure 2.1, the spacecraft has 2.8 eccentricity. It means the spacecraft is in hyperbolic orbit with respect to the Moon. Then, when the spacecraft is propagated for six days, the eccentricity changes to 0.7, meaning it has an ellipse orbit. In [19], it is explained that the shape of the LDRO changes with the distance to the Moon. The closer the spacecraft to the Moon, the more circular the orbit shape is.

Saying LDRO is Moon-centered is not entirely true. It is actually an Earth-centered orbit (Figure 2.2), except it is extremely perturbed by the Moon gravity. However, when looking at the orbit from an Earth-Moon rotating reference frame, the orbit can be seen as a Moon-centered orbit (Figure 2.1).

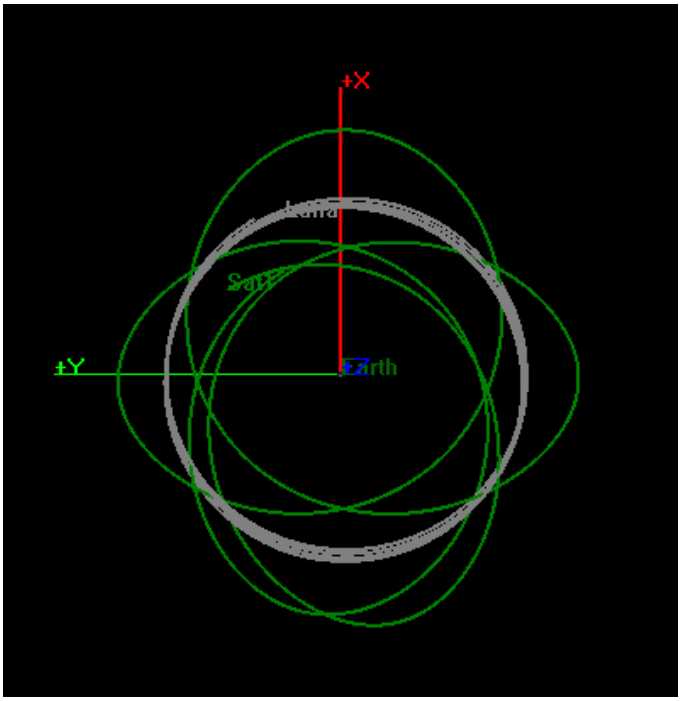


Figure 2.2: Lunar Distant Retrograde Orbit viewed from Earth-centered reference frame.

The LDRO was first documented by Broucke [20] in 1968. Furthermore, Murakami et al. [21] and Capdevila et al. [19] studied the trajectory design

from Earth to rendezvous in LDRO. These studies were motivated by the potential of putting a space station in LDRO. In [19], the motion of the spacecraft in CR3BP is represented by Equation 2.1

$$\ddot{x} - 2\dot{y} = \frac{\partial U}{\partial x}, \ddot{y} - 2\dot{x} = \frac{\partial U}{\partial y}, \ddot{z} = \frac{\partial U}{\partial z} \tag{2.1}$$

where $U$ is the pseudo-potential function. Equation 2.1 contains the position of the spacecraft, $[x, y, z]$, and the velocity, $[\dot{x}, \dot{y}, \dot{z}]$, in the rotating reference frame. Equation 2.2 is used to calculate the pseudo-potential function.

$$U = \frac{1}{2}(x^2 + y^2) + \frac{(1-\mu)}{r_{toEarth}} + \frac{\mu}{r_{toMoon}} \tag{2.2}$$

The $r_{toEarth}$ and $r_{toMoon}$ are measured from the spacecraft. The $\mu$ is the characteristic mass of Earth and Moon where $\mu = \frac{m_{Moon}}{m_{Earth}+m_{Moon}}$.

Such an orbit is not necessarily stable. Capdevila et al. [19] summarized the stability region for LDRO. However, all of the LDROs considered in the stability region are lower than 100 000 km distance from Moon-centered. Staying too close to Moon, increases the chance to crash on the Moon while simulating the Earth escape maneuver. Thus, a longer distance is desired. The LDROs reviewed by Turner [22] have a maximum distance of 120 000 km with a range of velocity vector to produce stable LDRO. Furthermore, according to [19], LDROs are only stable if 2-D motion is considered. Following the researches, a stable LDRO (Figure 2.1) at 125 000 km with slightly higher velocity than Turner's is found and used as the initial orbit of the spacecraft.

## 2.2 Capturing spacecraft to Earth-Moon System using Lunar Gravity Assist (LGA)

Gravity assist, a method of decreasing the required delta-V to reach a distant target, has been used numerously by past missions, such as Voyager [23], Mariner 10, Messenger [24], and New Horizons [25]. Using this method, Mariner 10 and Messenger successfully accessed the most inner planet in the Solar System, whereas, Voyager and New Horizons were able to reach the boundary of the Solar System. These achievements are only viable with the aid of gravity assist by the planets.

The mechanism of the gravity assist is fairly simple as explained in [26]. The spacecraft is in a hyperbolic trajectory with respect to a planet. The effect of the flyby is the hyperbolic excess velocity ($V_\infty$) direction of the spacecraft is changed. The heliocentric velocity of the spacecraft is then

increased/decreased affected by the planet heliocentric velocity. The mechanism can be easily understood in Figure 2.3.

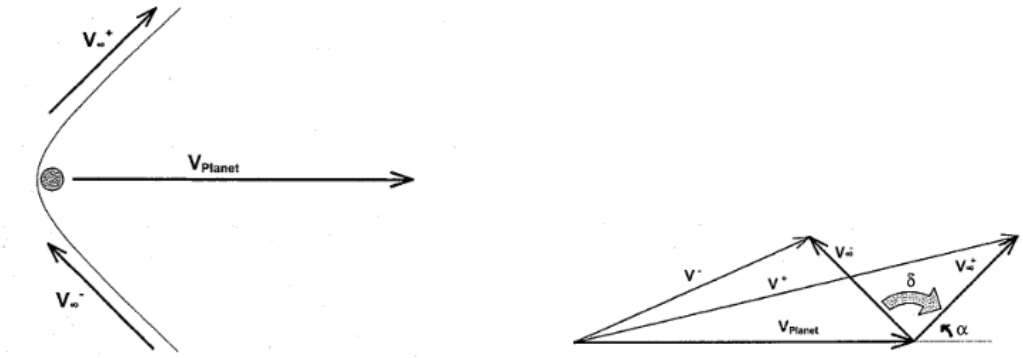


(a) Gravity assist schematic. (b) Gravity assist vector diagram.

Figure 2.3: Gravity assist mechanism [26].

Focusing on a small scale gravity assist, the Moon was used for helping missions to escape from the Earth-Moon system and to reach the Sun-Earth Liberation point. Uphoff [27] analyzed a Lunar gravity assist application in reaching L1 halo orbit. In addition, the ISEE-3/ICE mission [28] not only reached L1 halo orbit but also utilized Lunar gravity assist to encountered a comet called Giacobini-Zinner.

The LGA was planned to be utilized for NASA asteroid redirect mission. The spacecraft will approach Earth with a similar trajectory, then it will get pulled by the Earth gravity. Afterward, it will swing-by the Moon and get deflected to a loose Earth-centered orbit without a need for an insertion burn. The illustration of the concept is shown in Figure 2.4.

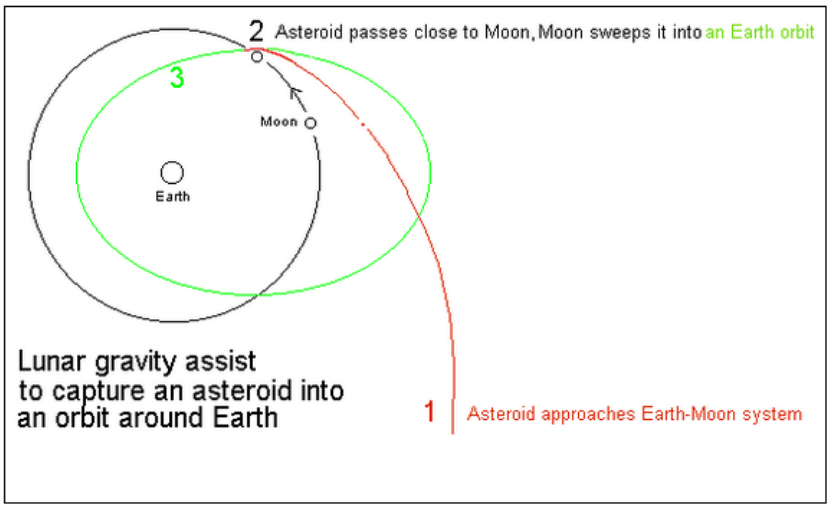


Figure 2.4: Illustration of the capture method using LGA [29].

## 2.3 Finite Burn

Impulsive burn has been used widely in a lot of simulations. It simplifies the maneuver of a spacecraft by assuming the changes on the velocity happens in an instant. Physically, none of the maneuvers is truly instantaneous. It is correct that most of the maneuvers are very short (in a fraction of seconds) and comparing them with the mission duration, the maneuver duration is not significant. In contrast, a finite burn takes into account the maneuver duration. The difference between impulsive and finite burn is shown in Figure 2.5.

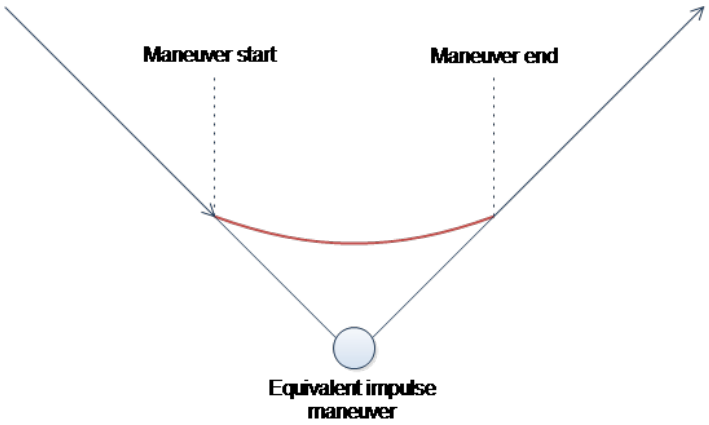


Figure 2.5: Illustration of the finite burn (red) and impulsive burn (circle).

The finite burn is usually used for a maneuver that needs precision, such as rendezvous maneuver with International Space Station. In this project, the finite burn is needed because the maneuver duration could exceed one day, which also implies the impulsive burn is not valid for the model.

## 2.4 Reference frames

Defining reference frames is critical in the model design. Reference frames used in the simulation is as follows.

1. Moon-centered, Earth-Moon rotating reference frame: the X-axis is parallel to the Moon orbit radius with respect to the Earth. The Y-axis is along the Moon velocity direction. The Z-axis completes the right-hand rule. The reference frame moves following Moon orbit around the Earth.

2. Earth-centered, Sun-Earth rotating reference frame: the X-axis is parallel to the Earth orbit radius with respect to the Sun. The Y-axis is along the Earth velocity direction. The Z-axis completes the right-hand rule. The reference frame moves following Earth orbit around the Sun.

3. Sun-centered, inertia reference frame: the axes are following J2000 axis system on ecliptic plane.

4. Spacecraft-centered, Sun-Spacecraft rotating reference frame: the X-axis is parallel to the spacecraft orbit radius with respect to the Sun. The Y-axis is along the spacecraft velocity direction. The Z-axis completes the right-hand rule. The reference frame moves following spacecraft orbit around the Sun.

# Chapter 3

# Methodology

This chapter explains the method used in designing the model and optimization.

## 3.1 Mission Design

### 3.1.1 Spacecraft Configuration

Before designing the mission, it is necessary to determine the spacecraft configuration. The spacecraft initially has 5000 kg dry mass and 5000 kg fuel mass. The spacecraft is equipped with a fuel tank that has a capacity of 100 000 kg. The spacecraft dimensions, however, are not determined because the solar wind pressure effect is assumed to be zero.

The maneuver is done by utilizing thrusters of up to 400 N for orbit transfer. The thrust vector of such thruster is varied by the optimizer. The $I_{SP}$ of the thruster is set to 370 s. Because the attitude of the spacecraft is not simulated, it is assumed that the spacecraft has thrusters installed in every thrust vector reference frame. The propellant used is a liquid type that can be re-fueled by the mining product.

In [33], the delta-v to deliver a 100 000 kg of fuel to Earth using chemical propulsion is studied. It takes 1 km s$^{-1}$ to 3 km s$^{-1}$ delta-v for a return trip to the Earth system. Using Newton's force equation as shown in Equation 3.1, the maneuver duration needed can be calculated. The maneuver needs up to 9 days burn to achieve the required delta velocity with 400 N thrust which cannot be represented by the impulsive burn model. Therefore, all maneuvers are considered in a finite burn model.

$$F = m * \frac{\Delta v}{\Delta t} \tag{3.1}$$

### 3.1.2 Mission Segmentation

The mission is divided into two parts. The first one is the departure from the Earth-Moon system. The spacecraft initially is in an LDRO, then it travels to the asteroid with a certain trajectory in a given time frame. Because the purpose of the thesis is to find the optimal fuel consumption, the departure time and the maneuver are included as the optimization variables.

The subsequent part is the arrival at the asteroid. The spacecraft is expected to rendezvous with the asteroid. However, the rendezvous process is not implemented and it is assumed that the rendezvous happens instantly after getting close to the asteroid below 100 km. The rendezvous fuel consumption, however, is taken into account by finding the delta-V of the spacecraft and the asteroid with respect to the Sun.

The spacecraft is required to stay near the asteroid for 92 days. This is due to the mining technology that the spacecraft will use. However, the launch window to Earth might not be present within the 92 days. Therefore, the mining duration is included as the optimization variables.

The return trip to the Moon can be divided into several phases. First, an asteroid escape maneuver and a Moon targeting maneuver. Both maneuvers result in a trajectory approaching the Moon. However, the C3 energy with respect to Earth could exceed $0\,\mathrm{km^2\,s^{-2}}$, which means the spacecraft is still in a hyperbolic trajectory with respect to Earth. Thus, LGA is utilized for capturing the spacecraft.

The LGA is characterized by several parameters, i.e., the distance between the spacecraft and the Moon, and the direction of the incoming trajectory. To maximize the LGA effect, the distance has to be close to the Moon. In this mission, less than 10 000 km is considered sufficient. Furthermore, according to Landau et al. [17], the spacecraft has to come with C3 energy less than $2\,\mathrm{km^2\,s^{-2}}$ and with inclination less than 30°, so that the spacecraft can be captured. Having low C3 energy at the LGA, allows the spacecraft to be placed at a smaller semi-major axis orbit. Furthermore, with low inclination, the subsequent orbit will also have a smaller inclination. This will lessen the spacecraft velocity in the Z direction, which makes the required fuel for the next phase lessen.

At this point, the spacecraft is already at an Earth-centered orbit, however, if the spacecraft is not moved from such orbit, it will leave the Earth-Moon system eventually. Muirhead et al.. [34], mentioned that it is essential to change the orbit into a more stable orbit. Thus, the next maneuver is planned to chase the Moon and finish far enough from the LDRO so that the spacecraft can do an LDRO injection maneuver. This location is then called the injection point. It is represented in the optimization constraint as the

X and Y components of the position vector with respect to Lunar-centered rotating frame. To control the incoming direction of the spacecraft, the velocity at injection point in Lunar-centered rotating frame is also restricted. This phase is called the second phase of the return trip.

The third phase of the return trip is the injection maneuver which has a purpose to put the spacecraft in the initial LDRO. The LDRO is defined by the position and velocity vector at a chosen location named entry point. However, targeting only position and velocity vectors is not enough to produce the initial LDRO, because the position of the Moon is not the same as where it was at the initial LDRO. Therefore, it is assumed that accomplishing the constraints would be enough for the actual control operation, later on, to alter the velocity so that the spacecraft can be easily placed in the LDRO.

The mission design is summarized in Figure 3.1.

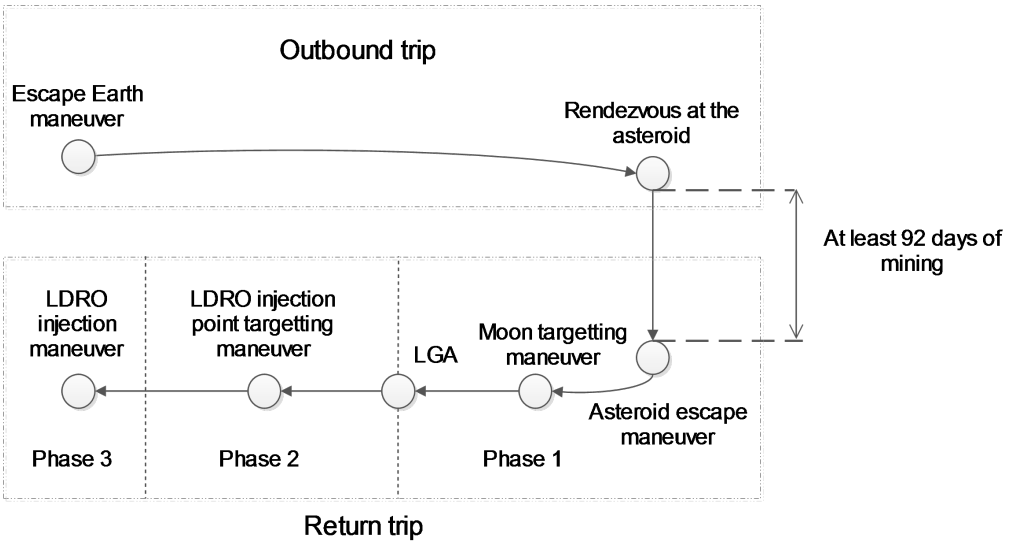


Figure 3.1: Mission design schematic.

## 3.2 General Mission Analysis Tool (GMAT)

The GMAT software was originally a private NASA software system for space mission analysis, trajectory optimization, and prediction [30]. The software then was released to the public as an open-source software. It is capable of simulating simple orbits and unconventional orbits such as LDRO and L2-centered orbit. It is currently used for supporting several missions, for instance, Solar Dynamics Observatory (SDO), Solar and Heliospheric Observa-

tory (SOHO), the Advanced Composition Explorer (ACE), Wind, Transiting Exoplanet Survey Satellite (TESS), and the Lunar Reconnaissance Orbiter (LRO) [31].

### 3.2.1 Spacecraft model

The GMAT software is capable of modeling a detailed spacecraft. The basic parameters are the spacecraft orbital elements which can be inputted as a Keplerian format or a Cartesian format. The epoch of the spacecraft needs to be loaded as well. If simulating solar wind pressure, or drag force is desired, it is important to fill in the dimension of the spacecraft and the specific parameters. Furthermore, GMAT is also able to simulate the attitude of the spacecraft. The example of the user interface is shown in Figure 3.2.

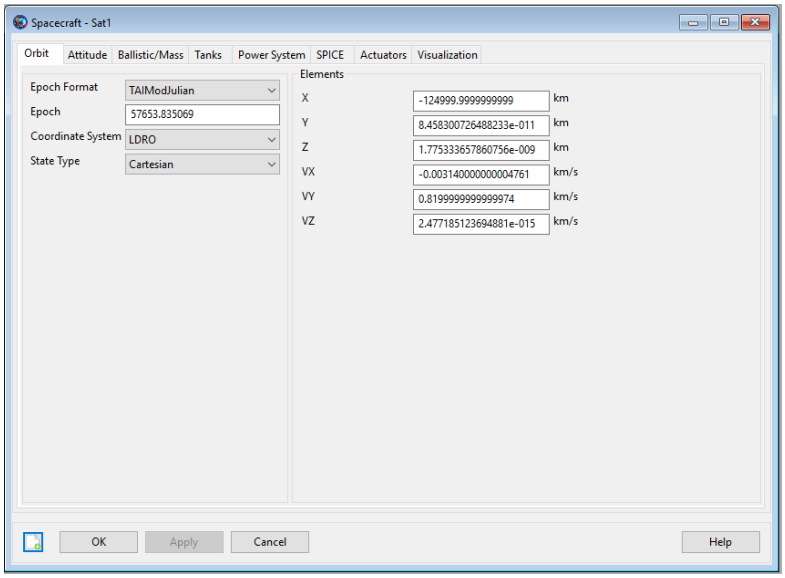


Figure 3.2: Spacecraft setting user interface.

In building the model, the solar wind pressure is assumed to be zero. Thus, the dimension is kept in the default value. To simulate a maneuver, the actuators and tanks are needed to be set properly. The tank volume is set to be $80\,\mathrm{m}^3$ which is enough to hold $100\,000\,\mathrm{kg}$ fuel with density of $1260\,\mathrm{kg\,m}^{-3}$. The $400\,\mathrm{N}$ thrusters are also installed on the spacecraft.

### 3.2.2 Thruster configuration

In a real-life mission, the spacecraft usually changes its attitude to move the thruster vector to the desired direction. In the model, the spacecraft attitude

is not included. Hence, the spacecraft needs to have different thrusters for each maneuver, because the reference frame is different for each maneuver.

The setting of the thrusters is shown in Figure 3.3. The important setting is the reference frame. There is a total of five maneuvers in the model. Each of the maneuvers reference frames is customized to match the current state of the spacecraft.

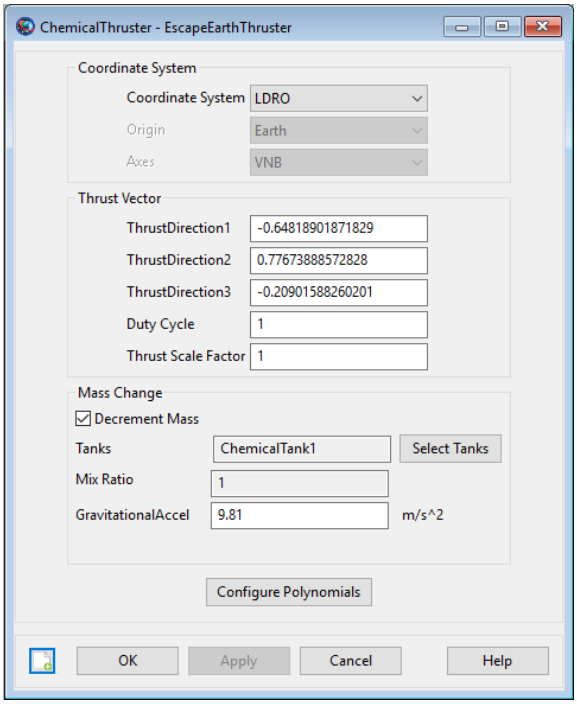


Figure 3.3: Thruster setting user interface.

### 3.2.3 Asteroid model

In GMAT, it is possible to add the asteroid as an astronomical object. The user interface is shown in Figure 3.4. However, the GMAT software needs an input file with a SPICE format [32]. This particular format is constructed from several elements.

**S**: spacecraft emphemeris as a function of time.

**P**: location of target astronomical object as a function of time.

**I**: scientific instrument specification.

**C**: information about the orientation of the spacecraft/instrument.

**E**: information about events or mission activities.

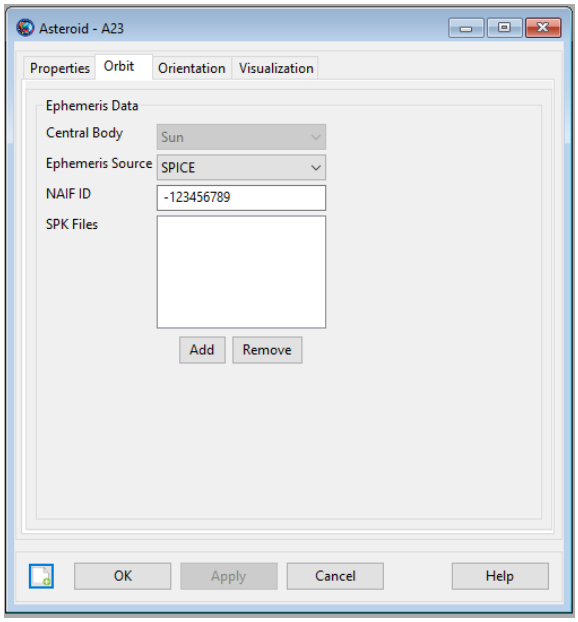


Figure 3.4: GMAT user interface for inputting asteroid data.

Because the database of the synthetic arjuna-type asteroids does not have SPICE format, the asteroid is inputted as a spacecraft. The dimension, weight, and other spacecraft physical parameters are kept as default, except, the orbital elements.

### 3.2.4 Propagator

The propagator is the highlight of GMAT. It is capable of solving three-body problem and allows the user to be able to simulate unusual orbits. The choices of the solver are quite complete. There are eight numerical integrators and three emphemeris-types that can be chosen as a solver. The default solver is "Runge-kutta89". The user interface is shown in Figure 3.5.

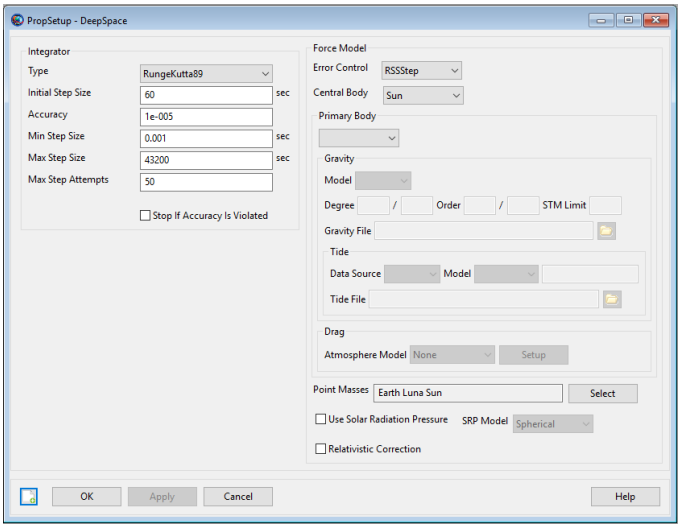


Figure 3.5: GMAT user interface for editing the simulation environment.

Another interesting section that deserves attention is the force model. It determines every force that works on the spacecraft such as solar wind pressure, drag, and gravity from astronomical bodies.

## 3.3 Optimization

### 3.3.1 Procedure

The model composes of four optimization steps as shown in Figure 3.6. The first one is the outbound trip optimization which focuses on finding a trajectory to the asteroid. The return trip is divided into three steps. This is due to the vast amount of the variables and constraints. First, the return trip phase one is optimized. Then, it is followed by phase two optimization. The last optimization is the combination of the whole return trip phases with the result of phase one and phase two optimization as the initial guesses.

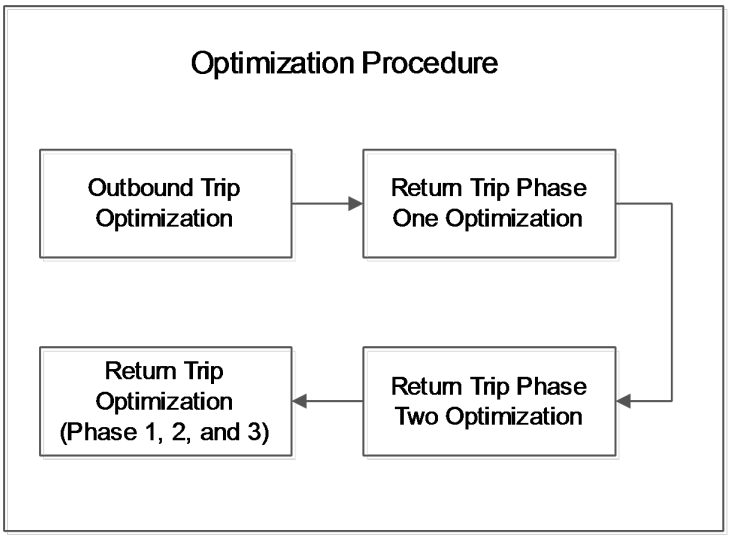


Figure 3.6: Optimization procedure schematic.

### 3.3.2 Optimizer - Matlab *fmincon*

MATLAB *fmincon* is a local minimum optimizer with a gradient-based method using a given algorithm. There are several choices of the algorithm in MATLAB, i.e. interior-point, trust-region reflective, sqp, and active set. The algorithm used by GMAT is active-set. It solves the problem by altering it into an easier subproblem which can be used as the base for the iterative process. MATLAB version 9.6 (2019) is using the solution of the Karush-Kuhn-Tucker (KKT) equations for this algorithm. The complete explanation is available in MATLAB documentation [35].

Two optimization method are considered for this research, the MATLAB genetic algorithm method and MATLAB *fmincon*. After comparing the performance of both optimization methods, *fmincon* has a big advantage in the duration to finish whether it is convergence or non-convergence. MATLAB genetic algorithm needs at least one day to finish, and MATLAB *fmincon* is able to finish maximum in 6 hours. Therefore, the MATLAB *fmincon* is chosen as the optimization method.

### 3.3.3 Variables, Constraints, and Objective Function

Selecting the correct variables and constraints are essential to produce the most optimum result. The variables and constraints will be separately explained according to the procedure mentioned in Section 3.3.1.

### Outbound Trip Optimization

Table 3.1 and Equation 3.2 show the variables and constraints used for the outbound trip.

Table 3.1: Outbound Trip variables.

| Variables | Lower Boundary | Upper Boundary |
|---|---|---|
| Escape Earth Thrust on X direction (N) | -400 | 400 |
| Escape Earth Thrust on Y direction (N) | -400 | 400 |
| Escape Earth Thrust on Z direction (N) | -400 | 400 |
| Escape Earth Maneuver duration (day) | 0 | 1 |
| Departure time (days) | 0 | 720 |
| Travel time to asteroids (days) | 0 | 720 |

In Table 3.1, the X, Y, Z direction of the thruster determine its vector. Because finite burn is utilized, the duration of the burn is needed for the model. Maneuver duration represents the duration of the propulsion burn. Thrust vector, burn duration, along with the travel time, shape the trajectory to the asteroid. Departure time affects the launch window opportunity which might be different for each asteroid. Thus, it gives the optimizer the flexibility to choose the launch time.

As mentioned in Section 3.1, the rendezvous is assumed to happen instantaneously after the spacecraft is less than 100 km distance to the asteroid. Therefore, the constraint needed is only the distance to the asteroid ($d_{toAst}$).

$$d_{toAst} \leq 100 \tag{3.2}$$

### Return Trip Phase One Optimization

Table 3.2 represents the variables used to define the mission in the return trip prior to LGA. The escape asteroid thrust direction, burn duration, and travel time 1, are used to form the trajectory. Before escaping the asteroids, the spacecraft needs to finish the mining process in at least 92 days. The remaining time, till the maximum 720 days, is the waiting time for the launch window. Moon target thruster, maneuver duration and travel time 2, are constructing the path that leads to Moon encounter.

Table 3.2: Return Trip Pre-LGA Variables .

| Variables | Lower Boundary | Upper Boundary |
|---|---|---|
| Escape Ast Thrust X direction (N) | -400 | 400 |
| Escape Ast Thrust Y direction (N) | -400 | 400 |
| Escape Ast Thrust Z direction (N) | -400 | 400 |
| Escape Ast Maneuver duration (days) | 0 | 5.157 |
| Mining duration (days) | 92 | 720 |
| Travel time 1 (days) | 0 | 720 |
| Moon Target Thrust X direction (N) | -400 | 400 |
| Moon Target Thrust Y direction (N) | -400 | 400 |
| Moon Target Thrust Z direction (N) | -400 | 400 |
| Moon Target Maneuver duration (days) | 0 | 5.157 |
| Travel time 2 (days) | 0 | 720 |

Table 3.3 shows the necessary constraints for phase one optimization. In section 3.1, it has been discussed the required constraints. Based on that, C3 energy at $0.5\,\mathrm{km^2\,s^{-2}}$ and inclination less than $10^\circ$ are determined for the optimizer constraints.

Table 3.3: Return Trip Pre-LGA Constraints.

| Constraints | Sign | Value |
|---|---|---|
| Distance to Moon (km) | $\leq$ | 10000 |
| The inclination to Ecliptic Plane (deg) | $\leq$ | 10 |
| C3 Energy ($km^2/s^2$) | $\leq$ | 0.5 |

### Return Trip Phase Two Optimization

In Table 3.4, Moon target 2 thrusters are the variables used to represent the spacecraft thruster for the maneuver in this phase. Together with the maneuver duration and travel time, produce trajectory to put the spacecraft at the injection point. The waiting time is to add flexibility for the optimization to find the best maneuver time.

Table 3.4: Return Trip Post-LGA Variables .

| Variables | Lower Boundary | Upper Boundary |
|---|---|---|
| Moon Target 2 Thrust X direction (N) | -400 | 400 |
| Moon Target 2 Thrust Y direction (N) | -400 | 400 |
| Moon Target 2 Thrust Z direction (N) | -400 | 400 |
| Moon Target 2 Maneuver duration (days) | 0 | 2.314 |
| Waiting for opportunity (days) | 0 | 300 |
| Travel time to Moon (days) | 0 | 300 |

Table 3.5 contains the constraints for the transition phase to the LDRO. All of the constraints are seen from Moon-centered Earth-Moon rotating frame. A suitable injection should not be far away from the entry point, thus the injection point X-component is given a leeway of 5000 km. The Y-component constraint ensures the injection point is always behind the entry point. The velocity vector constraints restrict the result so that the velocity at the injection point is not far different than the velocity at the entry point.

Table 3.5: Return Trip Post-LGA Constraints.

| Constraints | Sign | Value |
|---|---|---|
| X component magnitude (km) | $\leq$ | 5000 |
| Position Y component (km) | $\leq$ | -8000 |
| C3 Energy ($km^2/s^2$) | $\leq$ | -0.1 |
| Inclination to Moon-centered rotating frame (deg) | $\geq$ | 178 |
| Velocity in X direction (km/s) | $\leq$ | 0.15 |
| Velocity in X direction (km/s) | $\geq$ | -0.15 |
| Velocity in Y direction (km/s) | $\leq$ | 0.95 |
| Velocity magnitude (km/s) | $\leq$ | 0.95 |

### Combined Return Trip Optimization

The last optimization is the merger of phase one, phase two, and the injection maneuver. In total, there are 22 variables and 19 constraints. The variables used in the injection maneuver are shown in Table 3.6. It can be observed that the variables are very much similar to the previous phase. The only dissimilarity is the upper boundary of the variables. Because the spacecraft velocity has been limited with the constraints in the previous phase, the maneuver duration upper boundary is reduced to 150 000 s. The travel time upper boundary is also changed to 5 days, given the injection point and entry point is not far-off.

Table 3.6: LDRO injection maneuver variables.

| Variables | Lower Boundary | Upper Boundary |
|---|---|---|
| Injection Thrust X direction (N) | -400 | 400 |
| Injection Thrust Y direction (N) | -400 | 400 |
| Injection Thrust Z direction (N) | -400 | 400 |
| Injection Maneuver duration (days) | 0 | 1.736 |
| Travel time to Entry Point (days) | 0 | 5 |

The purpose of the constraints in Table 3.7 is to guarantee the spacecraft

is in the safe range for the control operation to successfully enter the LDRO. The position vector components X and Y are given a 500 km leeway. To make sure the component at Z direction is not more than 500 km, the vector magnitude and the position vector X component difference has to be less than 2. The velocity constraints are the condition when the spacecraft at the same point in the initial LDRO.

Table 3.7: LDRO injection maneuver constraints.

| Constraints | Sign | Value |
|---|---|---|
| Position X component (km) | $\leq$ | -124500 |
| Position X component (km) | $\geq$ | -125500 |
| RMAG to Moon (km) | $\geq$ | 124500 |
| RMAG to Moon (km) | $\leq$ | 125500 |
| RMAG and X component difference (km) | $\leq$ | 2 |
| Y component magnitude (km) | $\leq$ | 500 |
| Velocity in X direction (km/s) | $=$ | 0.022 |
| Velocity in Y direction (km/s) | $=$ | 0.774 |
| Magnitude of velocity in Z direction (km/s) | $\leq$ | 0.001 |

#### Optimization Objective Function

The objective function (ob) for all optimization is shown in Equation 3.3. The main purpose of the optimization is finding the most efficient maneuvers and trajectories. However, accomplishing the mission at the shortest amount of time is also desired. Both objectives, then, are combined with weight 75% and 25% for the fuel consumption (fc) and the mission duration (md) respectively.

$$ob = 0.75 * fc + 0.25 * md \tag{3.3}$$

### 3.3.4 Initial Guess

Another essential set of parameters are the initial guesses for the optimizer. The more complex a mission is, the more refined the initial guesses have to be. In this research, there is a big number of variables and constraints, which increase the complexity of the simulation.

The first approach is to look at the visualization of the spacecraft and the asteroid in the Sun-centered inertial reference frame. Then, by estimating the required time to reach such asteroid, the first initial guess for the travel time is generated. Estimating the velocity vectors and maneuver duration

using visualization is challenging. One possible approach are generating the initial guesses using random guess method.

The subsequent guesses are varied with the previous optimization progress as the basis. They are changed in a constant step size, typically around $1-5\%$ of the upper boundary. It is essential to not change more than two initial guesses at a time so that the behavior of all initial guesses can be observed completely.

It is also important to note that the result might not be close to the initial guesses. It is solely dependent on how the MATLAB *fmincon* finds the optimum trajectory. However, the results are always restricted by the boundary values of the variables.

### Refining Initial Guesses in the First Phase of the Return Trip

Estimating the initial guesses is a good alternative to the random guess method. One of the variables that can be estimated is the mining duration on the first phase of return trip optimization. The spacecraft needs to finish the mining process in at least 92 days. The following days are the waiting time for the launch window. In astrodynamics, the closer the spacecraft to the ascending/descending node, the better the maneuver can reduce the inclination. Thus, the initial guess for the mining duration is calculated as the time needed to encounter a node. As explained in Section 3.1.1, the spacecraft needs several days to change the velocity in the finite burn model. Thus, starting the asteroid escape maneuver with 4000 km distance to the node is considered.

The other variables are estimated by using logical reasoning. For instance, the first initial guess for travel duration is half of the spacecraft orbital period. It might not be true for all asteroids, but it is considered a good start for an initial guess. If the optimization fails, the initial guess of the travel time is increased/decreased until a good combination is found. To simplify the process of finding the correct initial guesses, the thrust direction and the maneuver direction initial guesses are fixed to certain values. There are two maneuvers utilized in the first phase. The first one is considered to have a big impact on the trajectory because this maneuver will reduce the inclination as much as possible and shape the path to the Earth system. Therefore, the initial guesses for such maneuver are set as a highly consuming maneuver with initial guess of the burn duration of 400 000 s. The second maneuver is considered as the trajectory correction maneuver which does not consume much fuel. The initial guess of its burn duration is set to 150 000 s. These initial guesses for the burn duration are not changed in the process of finding correct set of initial guesses.

The initial guess of the thrust vector, however, is changed based on the asteroid semi-major axis so that the resulting trajectory would intersect with the Earth's orbit. When the semi-major axis is bigger than Earth's, the initial guesses are set so that the spacecraft will decelerate which makes the resulting orbit smaller than the current orbit. Therefore, it will intersect with the Earth orbit. The velocity is accelerated if asteroid's semi-major axis is less than Earth's.

#### Refining Initial Guesses in the Second Phase of the Return Trip

During the second phase of the return trip optimization, the initial guesses can be estimated by looking at the visualization of the current orbit. The initial guess of the waiting time variable is estimated by finding the closest point of the spacecraft with respect to the Moon. Taking into account the finite burn model and the upper boundary of the maneuver duration, the maneuver is considered to start at least one day before the closest point.

The initial guess of velocity vector can be estimated by looking at the reference frame from the visualization. The initial guess of the maneuver duration, however, cannot be estimated accurately. It is intuitively guessed by looking at the current velocity direction. If the spacecraft velocity direction is far-off than Moon's velocity direction, the initial guess will be set to a high value, and vice versa.

#### Refining Initial Guesses in the Combined Return Trip Phases

The optimization consists of the first phase of the return trip, the second phase of the return trip, and the injection maneuver to the LDRO. The initial guesses for the first and second phase variables are set to the results from the previous optimization steps. The initial guesses of the injection maneuver is dependent on the result from the second phase of return trip. The velocity direction initial guess is set so that it can compensate the velocity difference between the injection point and entry point. The value of maneuver duration initial guess is intuitively guessed based on the velocity difference. The travel time initial guess is decided upon the distance between the injection point and the entry point.

### 3.3.5 Verification

Several asteroids are used to verify the model and optimization. Their orbital elements are presented in Table 3.8. These are synthetic Arjuna-type near-Earth asteroids which have low C3 energy which are taken from a database

consisting of more than 4000 asteroids. The chosen asteroids are varied in terms of the orbital elements to fully examined the optimization. It enables observation of the model capability to find optimized trajectory for the mission.

Table 3.8: Arjuna type asteroids used for verification of the optimization.

| Ast. Number | SMA | Eccentricity | Inclination | A.o. Perigee | RAAN | True Anomaly |
|---|---|---|---|---|---|---|
| 3 | 0.972 | 0.163 | 2.386 | 147.333 | 206.458 | 353.791 |
| 33 | 1.037 | 0.192 | 0.572 | 206.744 | 352.438 | 199.182 |
| 57 | 0.972 | 0.089 | 1.162 | 39.391 | 164.997 | 204.388 |
| 88 | 0.931 | 0.085 | 2.272 | 14.158 | 44.701 | 58.860 |
| 276 | 1.001 | 0.068 | 3.485 | 8.020 | 12.259 | 20.279 |
| 330 | 1.036 | 0.072 | 3.156 | 42.741 | 184.302 | 227.042 |
| 462 | 1.089 | 0.123 | 1.800 | 283.402 | 191.376 | 114.778 |
| 1136 | 0.999 | 0.040 | 2.475 | 227.676 | 89.222 | 316.897 |
| 1742 | 0.998 | 0.039 | 3.374 | 54.573 | 337.991 | 32.564 |
| 2624 | 0.888 | 0.029 | 1.554 | 154.115 | 325.059 | 119.174 |
| 3096 | 0.942 | 0.044 | 2.705 | 59.541 | 8.989 | 68.530 |
| 3474 | 1.066 | 0.087 | 2.791 | 9.838 | 41.824 | 51.661 |
| 3532 | 1.056 | 0.056 | 4.784 | 135.114 | 254.126 | 29.240 |
| 68 | 1.087 | 0.084 | 1.056 | 343.543 | 258.265 | 241.808 |
| 173 | 0.969 | 0.047 | 3.623 | 308.235 | 218.357 | 166.592 |
| 4160 | 1.162 | 0.050 | 2.606 | 298.042 | 257.110 | 195.153 |
| 1941 | 1.027 | 0.082 | 3.644 | 25.235 | 103.819 | 129.054 |
| 1289 | 1.053 | 0.168 | 0.786 | 21.174 | 258.578 | 279.753 |
| 2340 | 1.000 | 0.091 | 2.792 | 275.927 | 150.055 | 65.982 |
| 3665 | 0.982 | 0.145 | 0.484 | 68.992 | 190.289 | 259.281 |
| 267 | 1.006 | 0.133 | 1.403 | 223.600 | 124.437 | 348.037 |
| 905 | 0.991 | 0.061 | 0.742 | 45.500 | 180.588 | 226.088 |
| 300 | 0.996 | 0.052 | 2.416 | 218.402 | 63.576 | 281.978 |
| 2303 | 1.000 | 0.061 | 2.153 | 75.924 | 291.071 | 6.995 |
| 2501 | 1.000 | 0.040 | 2.164 | 121.196 | 246.893 | 8.089 |
| 596 | 0.992 | 0.060 | 1.562 | 50.192 | 184.311 | 234.502 |
| 2812 | 1.010 | 0.041 | 2.370 | 30.462 | 123.086 | 153.548 |

There is a possibility that the optimization is not able to find a path to the asteroid or back to Earth in several days. Thus, there is a time limit of two days for optimizing one asteroid. If the limit has passed, the optimization is considered failed to discover the trajectory to reach such asteroid.

# Chapter 4

# Results

The chapter contains the results from the optimization. The results are divided into three parts, the optimization status, fuel consumption, and mission duration.

## 4.1 Optimization status

Table 4.1 shows the status of the optimization. 'Finished' means the optimization succeeded to find the trajectories for both outbound trip and return trip. 'Failed' means the optimization cannot find the trajectories for either the outbound trip or return trip. Note that, the failure status is after trying several initial guesses to no avail. The failure is given an identifier to state which part of the optimization is failed.

Table 4.1: Optimization status of the asteroids.

| Ast. Number | Status |
|---|---|
| 3 | Finished |
| 33 | Failed at the second step |
| 57 | Finished |
| 88 | Finished |
| 276 | Finished |
| 330 | Finished |
| 462 | Finished |
| 1136 | Failed at the third step |
| 1742 | Finished |
| 2624 | Failed at the second step |
| 3096 | Finished |
| 3474 | Finished |

| Ast. Number | Status |
|---|---|
| 3532 | Failed at the second step |
| 68 | Finished |
| 173 | Finished |
| 4160 | Failed at the fourth step |
| 1941 | Failed at the second step |
| 1289 | Finished |
| 2340 | Finished |
| 3665 | Failed at the second step |
| 267 | Finished |
| 905 | Finished |
| 300 | Failed at the second step |
| 2303 | Finished |
| 2501 | Failed at the fourth step |
| 596 | Failed at the third step |
| 2812 | Finished |
| 1870 | Finished |
| 3135 | Finished |

## 4.2 Fuel consumption

Table 4.2 represents the fuel consumption for the round trip to the target asteroids. The fuel consumption is displayed in a mass unit (kilograms) so that it can be easily understood and compared. The symbol "-" means the optimization failed to find the trajectory to the asteroid. The ratio shows how big the difference between the outbound trip consumption and the return trip consumption.

Table 4.2: Fuel consumption to reach target asteroid.

| Ast. Number | Fuel Consumption(kg) | | Total(kg) | Ratio |
|---|---|---|---|---|
| | Outbound Trip | Return trip | | |
| 3 | 3788.710 | 58015.002 | 61803.712 | 15.313 |
| 33 | 2244.610 | - | - | - |
| 57 | 3293.995 | 44574.384 | 47868.379 | 13.532 |
| 88 | 3705.569 | 54897.832 | 58603.401 | 14.815 |
| 276 | 3015.495 | 55958.877 | 58974.372 | 18.557 |
| 330 | 4695.241 | 57126.180 | 61821.421 | 12.167 |
| 462 | 3654.192 | 55957.470 | 59611.662 | 15.313 |
| 1136 | 3749.250 | - | - | - |

| Ast. Number | Fuel Consumption(kg) | | Total(kg) | Ratio |
|---|---|---|---|---|
| | Outbound Trip | Return trip | | |
| 1742 | 1166.812 | 45304.963 | 46471.775 | 38.828 |
| 2624 | 1273.831 | - | - | - |
| 3096 | 3785.634 | 54265.855 | 58051.489 | 14.335 |
| 3474 | 1885.108 | 58463.030 | 60348.138 | 31.013 |
| 3532 | 2125.948 | - | - | - |
| 68 | 1981.991 | 53804.643 | 55786.634 | 27.147 |
| 173 | 3345.677 | 53523.252 | 56868.929 | 15.998 |
| 4160 | 4382.270 | - | - | - |
| 1941 | 4697.430 | - | - | - |
| 1289 | 1804.663 | 53367.294 | 55171.958 | 29.572 |
| 2340 | 4233.966 | 53290.913 | 57524.879 | 12.587 |
| 3665 | 4465.840 | - | - | - |
| 267 | 3413.808 | 52631.151 | 56044.959 | 15.417 |
| 905 | 2673.030 | 51527.252 | 54200.282 | 19.277 |
| 300 | 4208.770 | - | - | - |
| 2303 | 4310.972 | 45699.254 | 50010.226 | 10.601 |
| 2501 | 2105.098 | - | - | - |
| 596 | 3839.088 | - | - | - |
| 2812 | 4697.573 | 55601.260 | 60298.833 | 11.836 |
| 1870 | 4484.669 | 23578.742 | 28063.411 | 5.258 |
| 3135 | 4386.236 | 15579.282 | 19965.518 | 3.552 |

## 4.3 Mission duration

The mission duration is shown in Table 4.3. The symbol "-" represents the failed optimization. The ratio shows the difference between return trip duration and outbound trip duration.

Table 4.3: Mission duration for the targets asteroids.

| Ast. Number | Outbound Trip Duration (days) | Return Trip Duration (days) | Total Mission Duration (days) | Ratio |
|---|---|---|---|---|
| 3 | 792.2 | 462.7 | 1254.9 | 0.6 |
| 33 | 227.1 | - | - | - |
| 57 | 232.7 | 719.7 | 952.3 | 3.1 |
| 88 | 568.4 | 1964.0 | 2532.5 | 3.5 |
| 276 | 534.5 | 502.7 | 1037.2 | 0.9 |
| 330 | 586.6 | 375.0 | 961.6 | 0.6 |

| Ast. Number | Outbound Trip Duration (days) | Return Trip Duration (days) | Total Mission Duration (days) | Ratio |
|---|---|---|---|---|
| 462 | 715.4 | 527.6 | 1243.0 | 0.7 |
| 1136 | 545.8 | - | - | - |
| 1742 | 283.4 | 938.3 | 1221.8 | 3.3 |
| 2624 | 996.8 | - | - | - |
| 3096 | 545.4 | 1874.3 | 2419.6 | 3.4 |
| 3474 | 342.9 | 602.1 | 945.0 | 1.8 |
| 3532 | 223.8 | - | - | - |
| 68 | 549.3 | 763.7 | 1313.0 | 1.4 |
| 173 | 414.1 | 1105.7 | 1519.8 | 2.7 |
| 4160 | 352.4 | - | - | - |
| 1941 | 595.3 | - | - | - |
| 1289 | 818.9 | 1637.9 | 2456.8 | 2.0 |
| 2340 | 246.0 | 1615.5 | 1861.5 | 6.6 |
| 3665 | 791.9 | - | - | - |
| 267 | 562.5 | 1098.0 | 1660.5 | 2.0 |
| 905 | 566.1 | 863.2 | 1429.3 | 1.5 |
| 300 | 765.0 | - | - | - |
| 2303 | 277.0 | 977.6 | 1254.6 | 3.5 |
| 2501 | 415.5 | - | - | - |
| 596 | 560.4 | - | - | - |
| 2812 | 437.5 | 1470.2 | 1907.7 | 3.4 |
| 1870 | 659.1 | 2022.8 | 2681.9 | 3.1 |
| 3135 | 508.4 | 1985.2 | 2493.6 | 3.9 |

# Chapter 5

# Analysis and Discussion

## 5.1 Optimization Capability

The optimization was applied to asteroids in Table 3.8. There are 29 target asteroids that have been studied, and the overall failure rate for the optimization is 34%. The failure of an optimization step was due to its inability to converge into a solution while satisfying all the constraints. The failures happened only in the return trip in different steps. There are 6 failures on the second step, 2 failures on the third step, and 2 failures on the last step of the optimization. The status is summarized in Table 4.1.

The propagation model is capable of simulating the whole mission. Figure 5.1 shows the spacecraft trajectory in the outbound trip.


Figure 5.1: Spacecraft (blue) leaves the Earth system (green) and arrives at the asteroid(red).

In the return trip, the critical point is capturing the spacecraft using LGA. One example of LGA is shown in Figure 5.2. The spacecraft returns from an asteroid and gets deflected to an Earth-centered orbit.

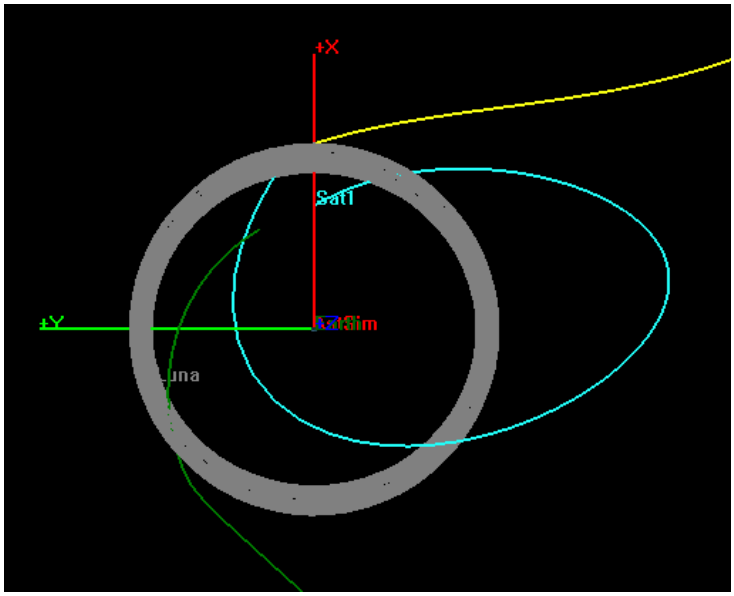


Figure 5.2: Spacecraft returns from an asteroid (yellow) and gets deflected to a high elliptical orbit (blue). The green trajectory is when the spaceraft leaves the Earth system.

In rare cases, the resulting orbits of LGA capture are not advantageous. For example in Figure 5.3, the spacecraft rendezvouses with the Moon after it passes the perigee. The spacecraft, then, cannot be deflected to a proper Earth-centered orbit. The spacecraft leaves the Earth system, however, it eventually comes back after more than 100 days with an almost 45° inclination.

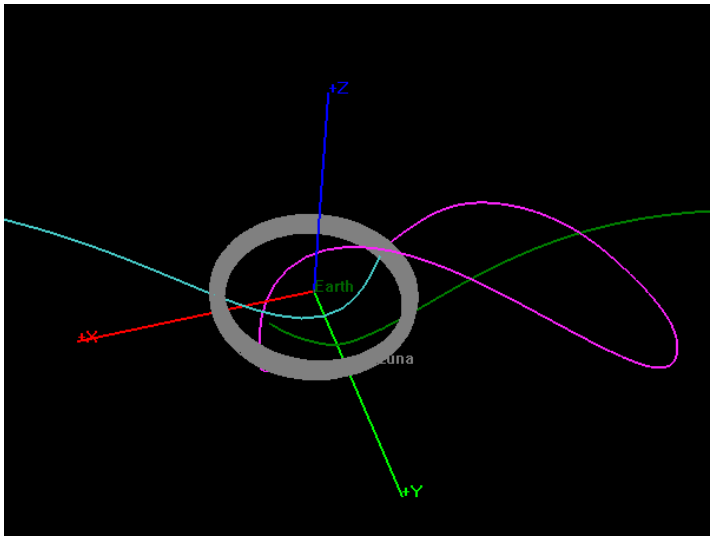


Figure 5.3: Spacecraft returns from an asteroid (blue) and it leaves the Earth after the LGA (pink).

In another case, the spacecraft does meet with the Moon before the perigee, however, the spacecraft is not captured properly which can be observed in Figure 5.4. The figure is taken from the failed optimization on the combined return trip.

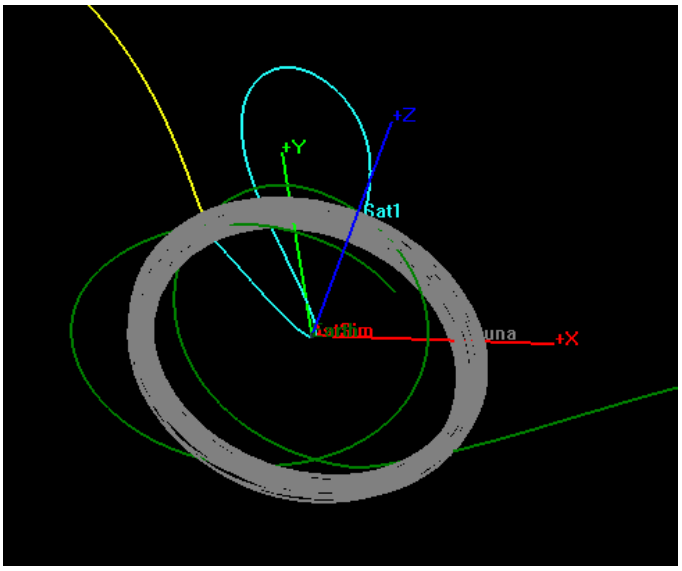


Figure 5.4: Spacecraft returns from an asteroid (yellow) and got deflected to an unexpected orbit (blue).

The odd orbits in Figure 5.3 and Figure 5.4 are the cause of the failure in the third step and the last step of the optimization. They have a small opportunity window to be placed in LDRO. There are five optimizations that result in these orbits, but only one that results in a convergence.

### 5.1.1 Outbound Trip

As shown in Table 4.1, the optimization successfully found a trajectory for each of the asteroids. Considering the asteroids orbital elements are diverse, the optimization has proven its capability in finding trajectories for many asteroids. In the early phase of the thesis, the random guess method was used for the initial guesses, however, it was difficult to achieve convergence. The method, then is changed and refined to decrease the difficulty.

The 100% success rate of the outbound trip is due to two factors. The first one is rendezvous with the asteroid is assumed to finish in an instant. Therefore, it simplifies the model. If the rendezvous model was added, the solution space would become narrower, which would make finding the trajectory more challenging. The other reason is the initial condition of the spacecraft is unchanging in each simulation. Due to this reason, a common set of first initial guess is found after many attempts in different asteroids and these initial guesses have a high success rate. The values for each variable are represented in Table 5.1.

Table 5.1: A first initial guess for the outbound trip.

| Variables | Initial Guess |
|---|---|
| Escape Earth Thruster X direction | -0.5 |
| Escape Earth Thruster Y direction | 1 |
| Escape Earth Thruster Z direction | 0.1 |
| Escape Earth Maneuver duration (secs) | 40000 |
| Departure timing (days) | 50 |
| Travel time to asteroids (days) | 200 |

The Y component of the velocity vector in the Moon-centered rotating frame is set to 1 and the X component is set to $-0.5$. The Y component is the direction of the Moon velocity with respect to Earth and the X component is parallel to the position vector of the Moon with respect to the Earth. The spacecraft will get accelerated in the same direction as the Moon's velocity. A sample of the trajectory can be seen in Figure 5.5.

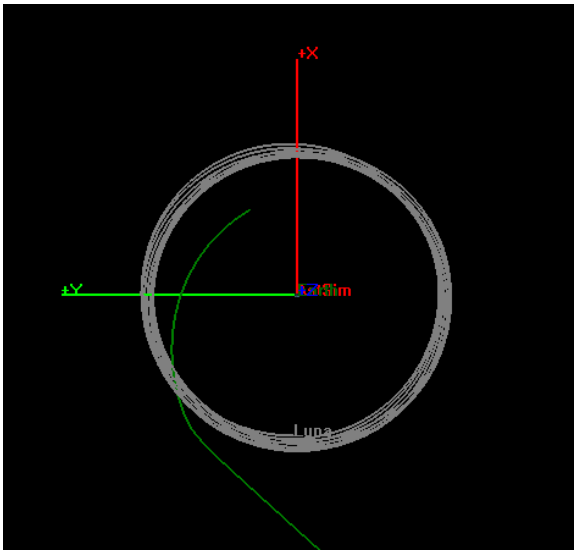


Figure 5.5: Spacecraft (green) leaves the Earth-Moon system in the direction of the Moon (grey) orbit.

The important note is that the common first initial guesses do not guarantee a convergence. For some of the asteroids, the initial guesses need to be altered to reach convergence. The common initial guesses are capable to converge on the first try with asteroid number 88, 276, 3096, and 3474. The mentioned asteroids have similar total values of the argument of perigee, right ascension ascending node, and true anomaly which is around 100°. The combination of the first initial guesses is also tested with a bigger total value such as asteroid number 1742's, and 3532's. Both optimizations of such asteroids succeeded to find the trajectory, however, they failed on the first attempt to achieve convergence. A convergence is found after the initial guess for the maneuver duration is increased. Furthermore, theses initial guesses was applied to 29 asteroids with 100% success rate to achieve convergence by only changing the maneuver duration initial guess.

### 5.1.2 Return Trip

After passing the checkpoint of the outbound trip, the optimization needs to find the trajectory for the return trip. There are 22 variables in total which make the success rate of finding the combination of the initial guesses that can produce a convergence is very low. Finding a first guess for 22 variables which works for a lot of asteroids is not an easy task either, because the initial position of the spacecraft at the return trip is different for each asteroid.

The establish solution is to separate the first and the second phase of the

return trip to two optimization. After the optimization of first and second phase are finished, the last optimization is the combination of all return trip phases. The results of segment one and segment two of the return trip optimization are then inputted as the initial guess for the last optimization variables. It significantly reduces the difficulty to get the result of the return trip.

Physically, there will always be a trajectory from one point to another point in space. Hence, the six failures on the first phase of return trip optimization are caused by the initial guesses of the variables. Although the initial guesses have been estimated properly, the optimizer cannot hold the values and will deviate them based on its algorithm. When the initial guesses are bad, the values of the variables deviate so much that the optimization fails to satisfy the constraints as shown in Figure 5.6.

| Control Variable | Current Value | Last Value | Difference |
|---|---|---|---|
| Sat1.EscAstThruster.ThrustDirection1 | -786.443605547883 | -786.443605547883 | 0 |
| Sat1.EscAstThruster.ThrustDirection2 | 786.4436055478834 | 786.4436055478834 | 0 |
| Sat1.EscAstThruster.ThrustDirection3 | -786.4436055478826 | -786.4436055478826 | 0 |
| escAstBurnDuration | -784.4436055478873 | -784.4436055478873 | 0 |
| return_m | -13.25782158888684 | -13.25782158888684 | -1.776356839400251e-15 |
| mining | 78.74217841111314 | 78.74217841111314 | 0 |
| Sat1.chasingMoon.ThrustDirection1 | -786.4436055478833 | -786.4436055478833 | 0 |
| Sat1.chasingMoon.ThrustDirection2 | 596.4791784328014 | 596.4791784328014 | 0 |
| Sat1.chasingMoon.ThrustDirection3 | 786.4436055478833 | 786.4436055478833 | 0 |
| chasingMoonBurnDuration | -784.4436055478873 | -784.4436055478873 | 0 |
| timeToMoon | -13.25782158888681 | -13.25782158888681 | -3.552713678800501e-15 |
| **Constraints** | **Desired** | **Achieved** | **Difference** |
| (==) lunaRMAG1 | -1 | -1 | 0 |
| (==) Sat1.EclipticEC.INC | -1 | -1 | 0 |
| (==) C3energy1 | -1 | -1 | 0 |
| (<=) lunaRMAG1 | 10000 | 37445994.31265667 | 37435994.31265667 |
| (<=) Sat1.EclipticEC.INC | 10 | 178.3729482675536 | 168.3729482675536 |
| (<=) C3energy1 | 0.5 | 67.27721620599698 | 66.77721620599698 |
| **Objective Function** | **Current Value** | **Last Value** | **Difference** |
| Cost | 92 | 92 | 0 |

**NO CONVERGENCE**
Optimization did not converge in 37 passes through the Solver Control Sequence

Figure 5.6: One example of a failed optimization.

As mentioned in Section 3.3.4, the thrust vector, the maneuver duration, and the mining duration initial guesses are not changed during the process of finding a proper initial guesses. The travel time are varied if the optimization is unable to converge. After changing the initial guess of the travel time, the new combination might have a potential to converge.

The process of finding a convergence was very challenging because even a difference of 1 day in the travel time initial guess, could change the convergence potential. If none of the initial guesses is unchangeable, the amount of combinations that could be tried to the optimization is enormous. Therefore, it can be said that the optimizer used is heavily dependent on the initial

guesses and an optimizer which does not depend much on initial guess could be a good alternative.

## 5.2 Analysis on the Fuel Consumption and the Mission Duration

### 5.2.1 Outbound Trip - Fuel Consumption

Observing Table 4.2, the smallest minimum fuel consumption is the trip to asteroid 1742 with 1166.8 kg. The results of other asteroids vary between 1273.8 kg and 4697.5 kg. Logically, the fuel consumption must be affected by the orbital elements of the asteroids. Therefore, the relations with the orbital elements are represented in several figures below. The first element studied is semi-major axis in Figure 5.7.

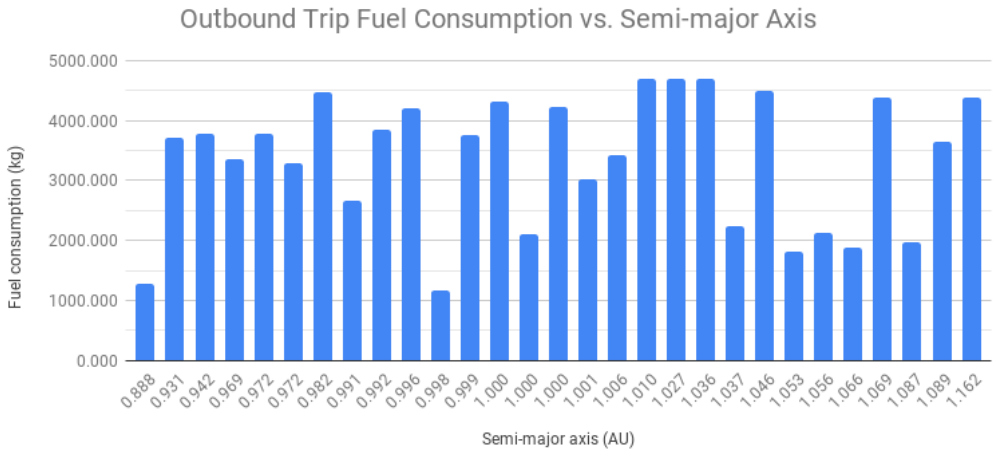


Figure 5.7: Fuel consumption relation with semi-major axis in the outbound trip.

In Figure 5.7, it can be observed that there is a faint pattern around the Earth semi-major axis. The fuel consumption is lower when the semi-major axis is close to the Earth's, and it increases when it is far from the Earth's. However, some of the results do not follow the pattern. It indicates that there are other factors affecting the fuel consumption. One possibility is the position of the asteroids which is studied in Figure 5.8.

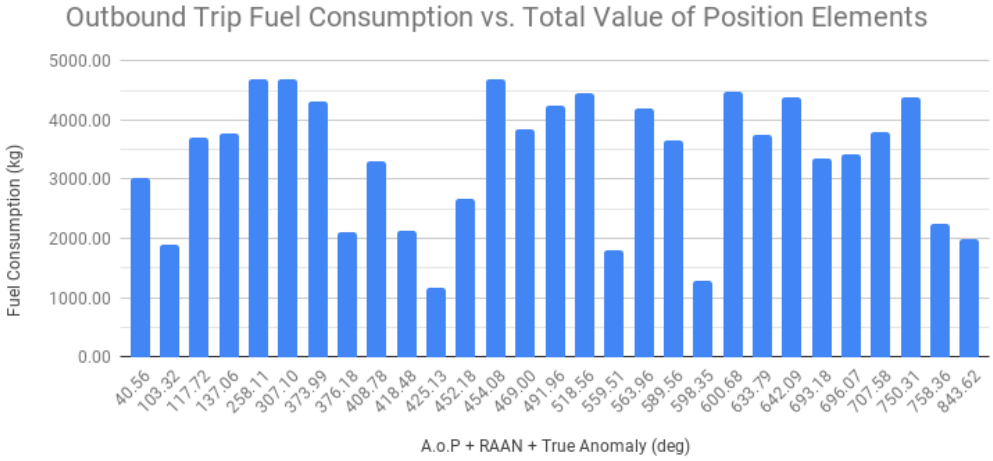


Figure 5.8: Fuel consumption relation with position orbital elements.

There is a noticeable pattern in Figure 5.8 when the values of position elements are around 420°. The fuel consumption is the lowest at 425.13°. This might be because the position of the asteroid and Earth are close to each other. To confirm the doubt, Figure 5.9 shows the asteroid and the Earth position in the Sun inertial reference frame. It is clear that the asteroid is close to the Earth.

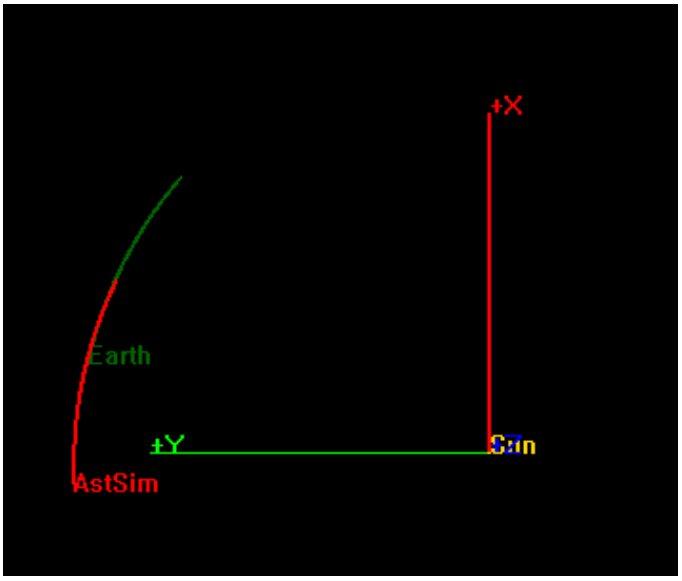


Figure 5.9: Position of asteroid 1742 with 425.13° total position elements and Earth in the Sun inertial reference frame.

The highest fuel consumption can be observed at 258.11° and 307.10°. It must be because the asteroids are behind the Earth which results in a longer distance to reach such asteroids. One of the asteroid's location is studied in Figure 5.10. It is clear that the asteroid is located behind the Earth.

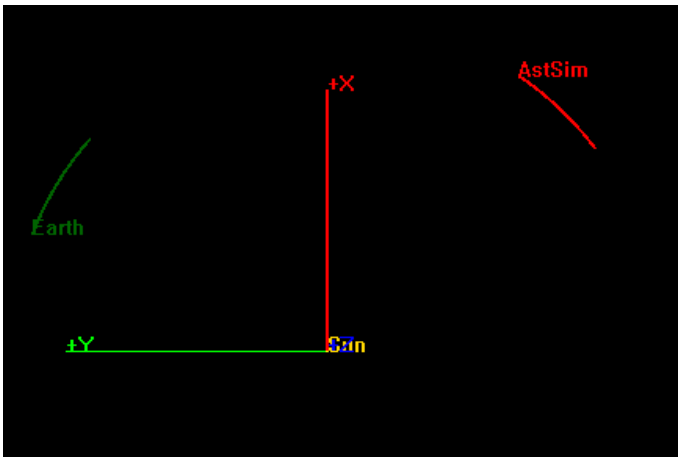


Figure 5.10: Position of asteroid 2812 with 307.10° total position elements and Earth in the Sun inertial reference frame.

One more interesting data in Figure 5.8 is at 598.3° and 600.68°. A difference of mere 2° could have more than 3000 kg gap in the fuel consumption. To investigate, the initial position and the trajectory of asteroid that has a 598.3° total value of position elements are visualized in Figure 5.11. The starting location of asteroid 2624 is about 180° away from the Earth (Figure 5.11a), but when the asteroid meets the spacecraft (Figure 5.11b), the position of the asteroid moves to several degrees away in front of the Earth. This is possible because asteroid 2624 has the smallest semi-major axis from the 29 asteroids. The closer a body to the Sun, the faster the velocity of such body orbiting around the Sun. The result of this particular optimization shows that the spacecraft waits for hundreds of days for launch window opportunity. This waiting time results in the asteroid position with respect to the Earth changed to be closer to the Earth which affects the fuel consumption.

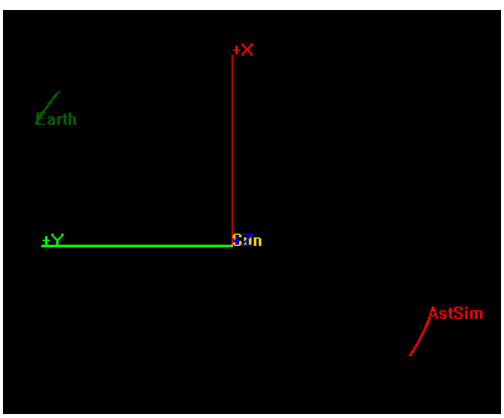


(a) Position of asteroid 2624 at starting point.

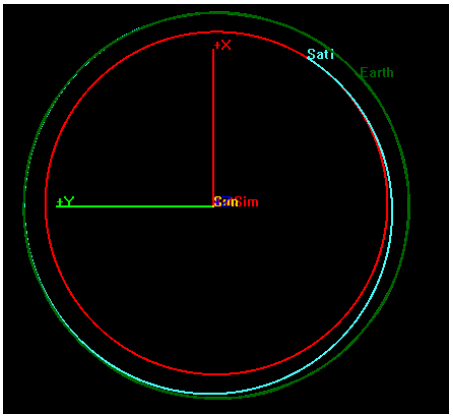


(b) Position of spacecraft when it meets asteroid 2624.

Figure 5.11: Position of asteroid 2624 in two situations.

Another important orbital element is inclination. The effect of inclination is that the Earth and the asteroids do not revolve around the Sun on the same plane. It makes the rendezvous opportunity smaller, because one of the constraint is the inclination to the ecliptic plane. The comparison of inclination and fuel consumption is shown in Figure 5.12.

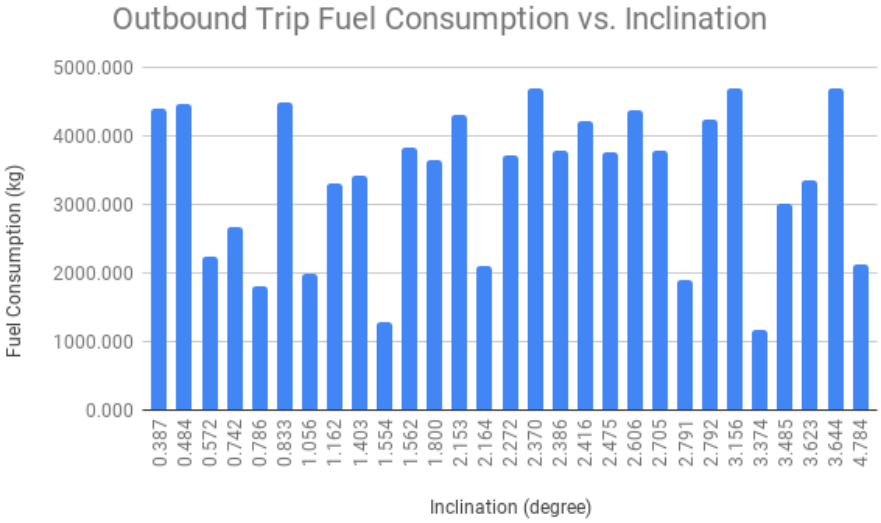


Figure 5.12: Fuel consumption relation with inclination.

Observing Figure 5.12, there is a vague pattern that the fuel consumption increases when the inclination increases. Logically, when the spacecraft and

the asteroids are not on the same plane, the spacecraft would need more fuel to reach the asteroid, because it is located further away than the zero inclination orbit. However, there are many deviations in the data. This means that the inclination is not the main factor in fuel consumption.

The eccentricity is also studied but there is no useful pattern on the data. Considering all the analysis from the previous paragraphs, there is no prominent effects from the asteroid orbital elements, except the position of the asteroids. Therefore, position of the asteroid can be acclaimed as the important factor to have a low fuel consumption.

### 5.2.2 Outbound Trip - Mission Duration

The longest duration for an outbound trip is an arrival time of 996.8 days at asteroid 2624. The reason has been explained in Section 5.2.1 that the spacecraft waited for hundreds of days for launch window opportunity. In contrast, the shortest duration is 223.8 days to reach asteroid 3532. As mentioned in Section 5.2.1, the closest asteroid position is when the total position elements around 400°. Asteroid 3532 is indeed close to Earth with 418.48°. The relation of the orbital elements with mission duration is studied in the figures below.

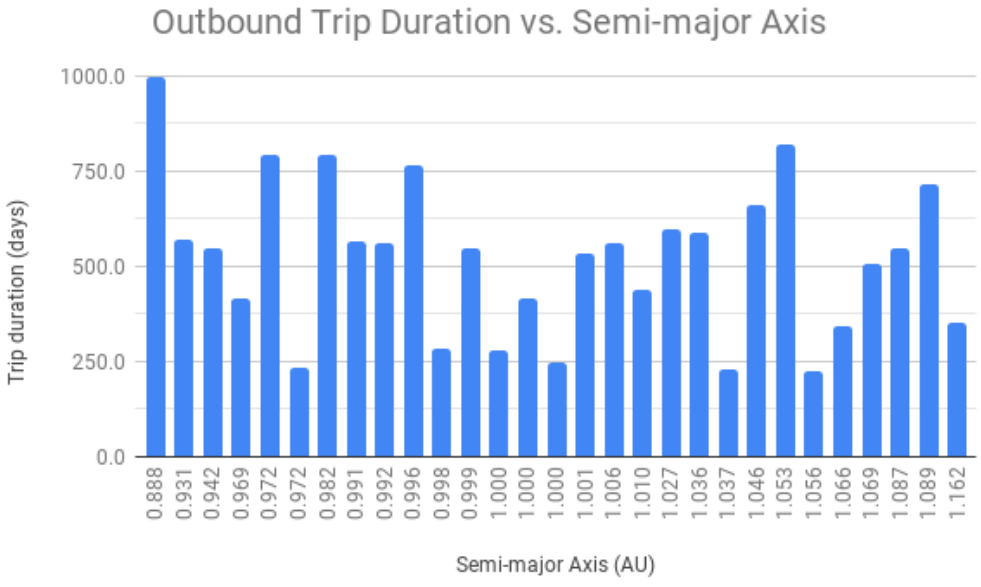


Figure 5.13: Mission duration relation with asteroids semi-major axis.

There is a faint pattern that the duration is short around 1 AU in Figure

5.13. The deviations in the data indicate that the other orbital elements affect the mission duration. This statement is evaluated by looking at asteroid 33 with 1.037 AU and asteroid 3532 with 1.056 AU. These asteroids have a low mission duration despite having a big semi-major axis. Asteroid 3532 has a total position elements value of 418.480° that is near the closest point to Earth. In addition, asteroid 33 has a total position value of 758.365°. At a glance, the difference is very big to the closest point, however, if the 400° is added by one full circle (360°), the asteroids are actually closer to one another. To investigate further, the relation between mission duration and the position of the asteroids are investigated in Figure 5.14.

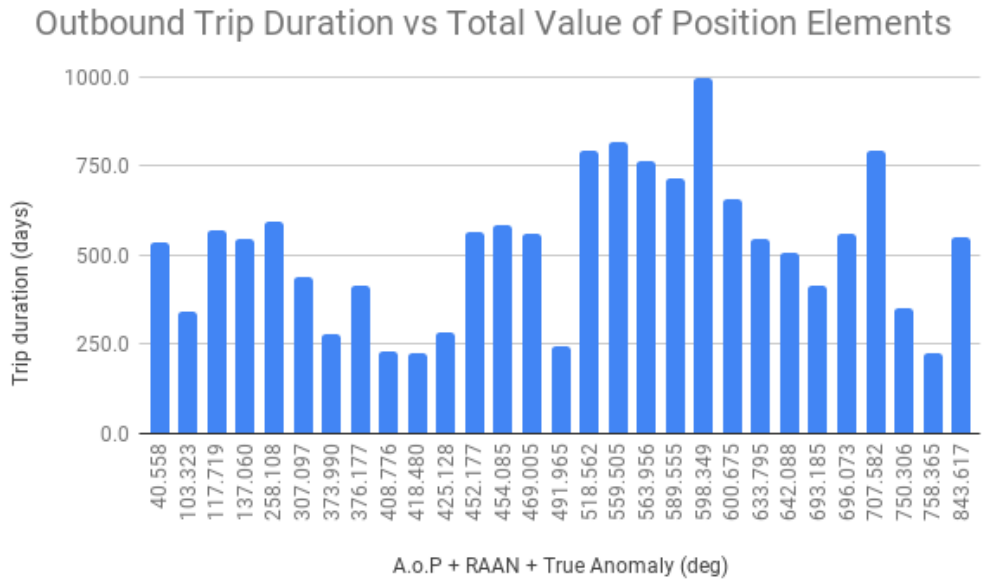


Figure 5.14: Mission duration relation with asteroids total value of the position elements.

It can be easily observed in Figure 5.14, that the duration is shorter around 400°. Then, it increases as the total value of position elements rise which indicates the asteroids are further away from Earth. One unusual value is asteroid 2624 with 598.349°. The reason is explained in the first paragraph of this subsection.

### 5.2.3 Return Trip - Fuel Consumption

The return trip is the biggest challenge for this thesis. The spacecraft has to bring 100 000 kg of fuel from an asteroid. According to [33], the maximum fuel

left after the spacecraft reach Earth system is 70% of the initial fuel mass and it is possible to consume as high as 60% of the initial fuel mass. Observing Table 4.2, the highest minimum fuel consumption is 58 463.0 kg, 58.46% of the initial fuel and the lowest minimum fuel consumption is only 15 579 kg, 15.579% of the initial fuel mass. The 58.46% fuel consumption is not ideal from a commercial point of view, but it is in the range of expectation. In contrast, 15.57% is beyond expectation and it is extremely convenient for commercial application. The more fuel left at the end of the mission, the more profit can be earned. The study in [33] is done by using a trajectory called broken-plane maneuver. However, the trajectory used in this project is found by the optimization. Therefore, it is possible to have such a low fuel consumption.

Most of the results are between 44 000 kg and 58 500 kg, except asteroid 1870 and asteroid 3135. The comparison of the fuel consumption and the orbital elements are then compared to find what makes asteroid 1870 and 3135 unique.

Figure 5.15 demonstrates the relation between the semi-major axis and the fuel consumption. The data point is not as many as the outbound trip, because all failures happened in the return trip optimization. Despite that, there is a hint of low fuel consumption near 1 AU but most of the asteroids consume more than 50 000 kg.

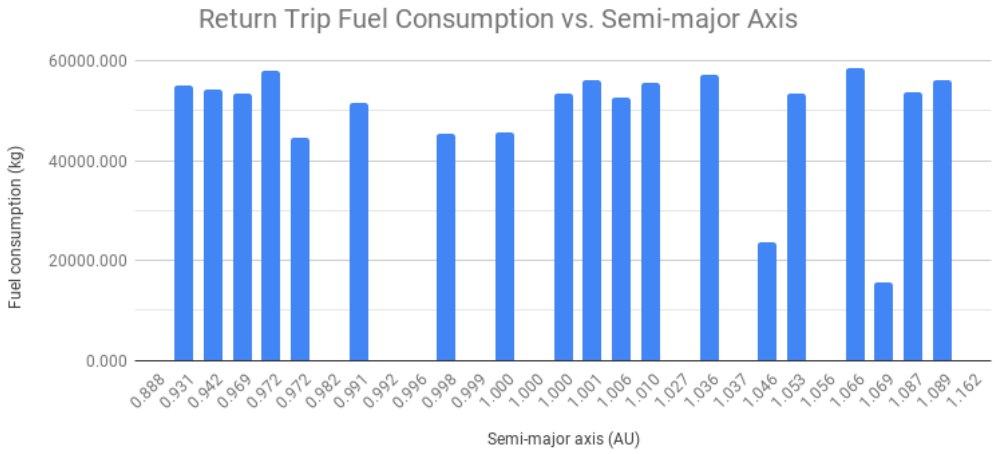


Figure 5.15: Fuel consumption relation with asteroids semi-major axis.

Interestingly, the two asteroids with very low fuel consumption are not anywhere near 1 AU. One possibility is that the asteroids are located close to the Earth. Thus, the total values of their position elements are investigated

in Figure 5.16.

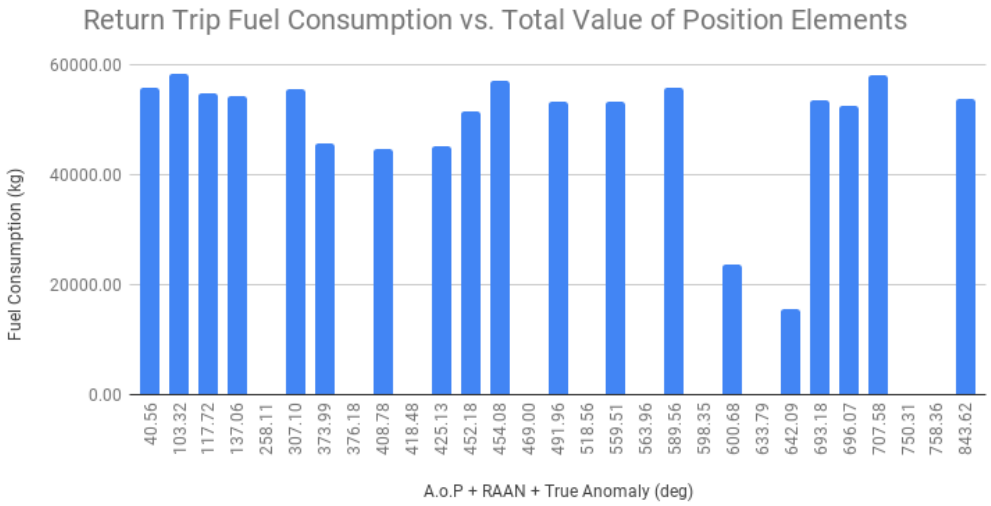


Figure 5.16: Fuel consumption relation with asteroids total values of position elements.

In the figure, it is clearly visible that both position values are close to each other, which are 600.68° and 642.09°. To confirm the suspicion that the asteroids are located close to the Earth, the visualization of their orbits is investigated. Asteroid 1870 with 600.68° and asteroid 3135 with 642.09° are shown in Figure 5.17.

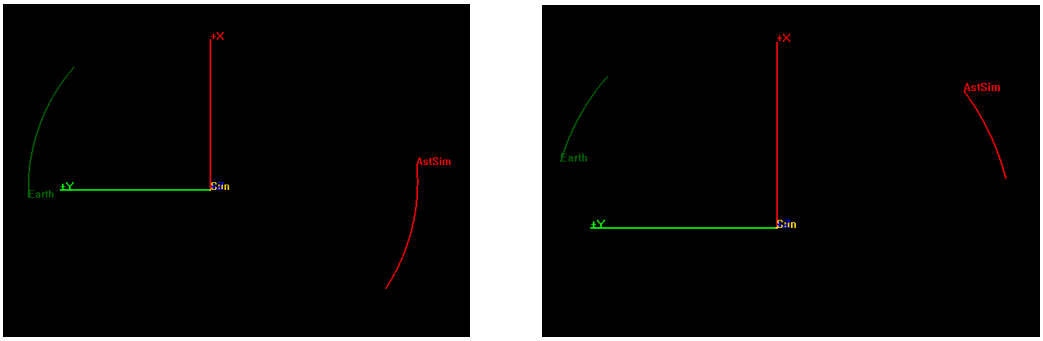


(a) Position of asteroid 1870.

(b) Position of asteroid 3135.

Figure 5.17: Position of asteroid 1870 and asteroid 3135 in Sun inertial reference frame.

The asteroids are not as close as expected to the Earth. It is rising a doubt

that there are other elements affecting the result. To expand the analysis, the inclination of the asteroids is studied in Figure 5.18.

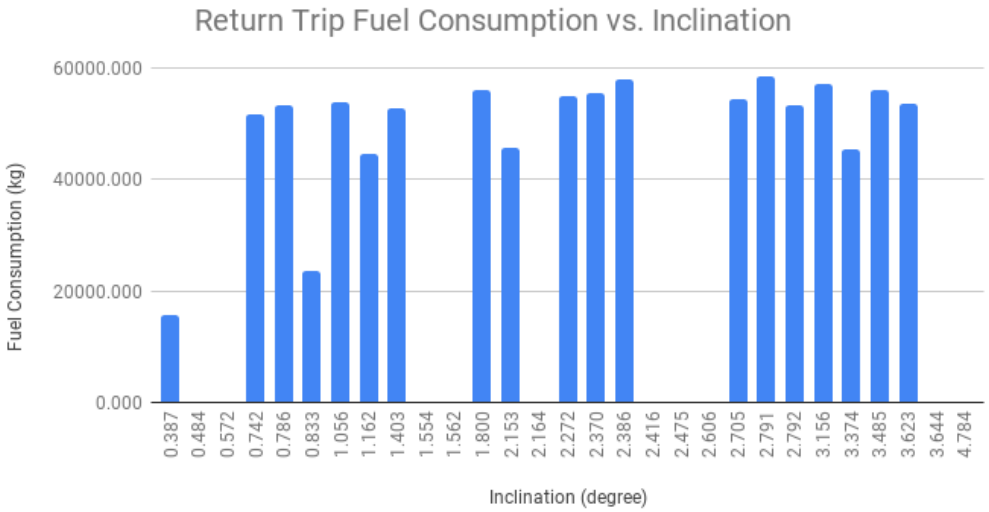


Figure 5.18: Fuel consumption relation with asteroids inclination.

From the figure above, it can be noted that the asteroid with the lowest inclination has the lowest fuel consumption. Furthermore, both asteroid 1870 and 3135 have inclination below 1°. However, there are two asteroids which have inclination below 1° with fuel consumption more than 50 000 kg. Comparing their orbital elements, one of the asteroids (asteroid 905) has a clear difference in the position with respect to the Earth. It is located approximately 45° in front of the Earth, which results in a very far distance for the return trip. The other asteroid (asteroid 1289) does not have a noticeable distinctness from asteroid 1870 and asteroid 3135. It opens a possibility that there is an external factor affecting the result.

### 5.2.4 Return Trip - Mission Duration

The mission duration for the return trip is diverse. The shortest duration is the time needed to come back from asteroid 330, which is 375 days. In contrast, the longest duration needed is 2022.8 days from asteroid 1870. Comparing the asteroids orbital elements, a clear difference is seen at their inclination and the position elements. The investigation of the effect of inclination to the mission duration is shown in Figure 5.19.

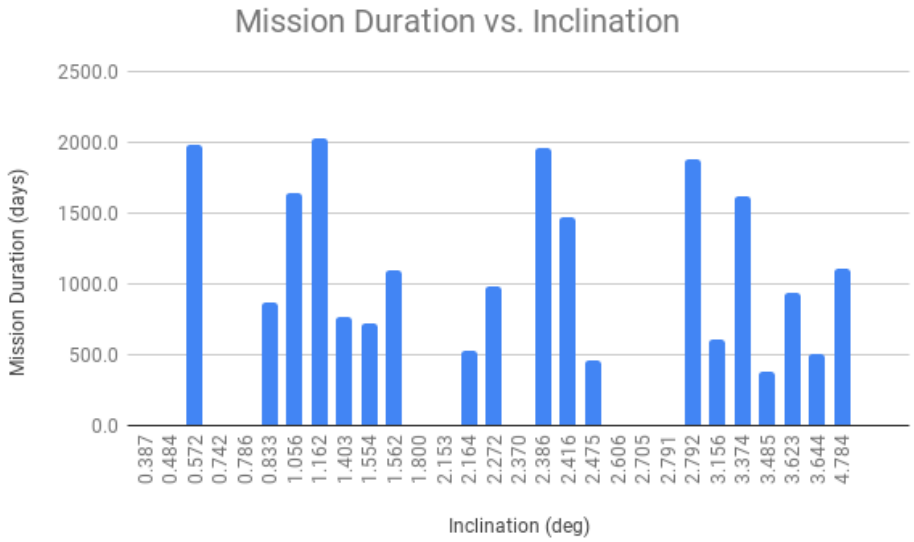


Figure 5.19: Mission duration relation with asteroids inclination.

It can be observed that there is no noticeable pattern in Figure 5.19. It means that several degree difference of the inclination does not contribute much to the results. The next factor worth investigating is the position of the asteroids which is shown in Figure 5.20.

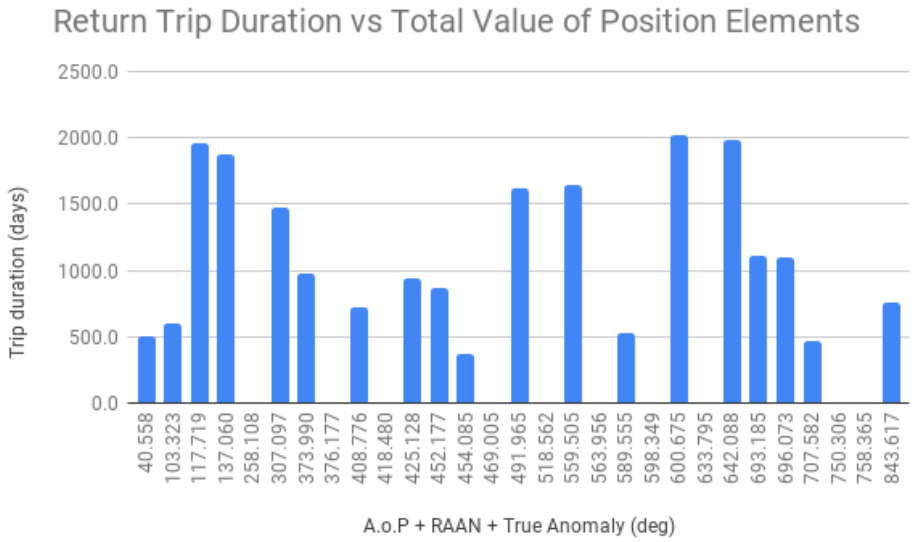


Figure 5.20: Mission duration relation with asteroids position elements.

In Figure 5.20, it can be observed there is a pattern in the data. However, there are some abnormal changes, for instance the second and the third data point. The duration increases from around 500 days to almost 2000 days over 14° difference on the position elements. This is only possible if the Earth is located between these asteroids. To check the suspicion, Figure 5.21 shows the position of the asteroids (asteroid 3474 and asteroid 88) in the Sun inertial reference frame.

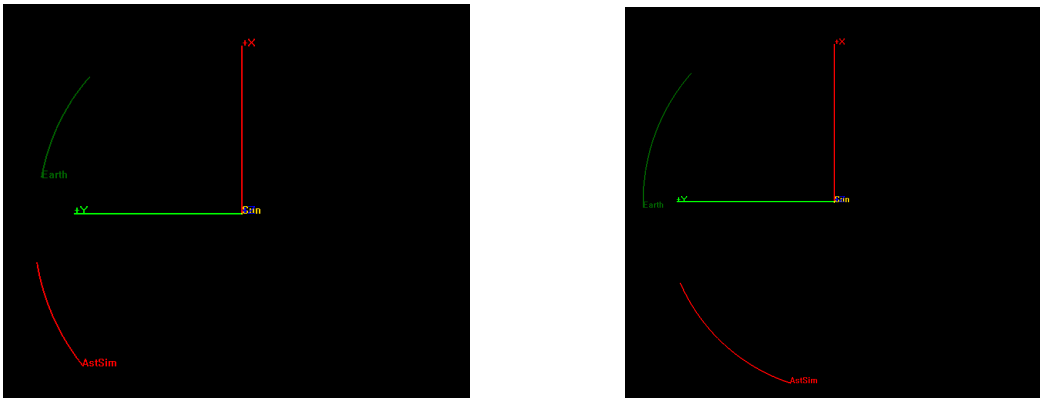


(a) Position of asteroid 3474.

(b) Position of asteroid 88.

Figure 5.21: Position of asteroid 3474 and asteroid 88 in Sun inertial reference frame.

In contrast to the suspicion, both asteroids are located in front of the Earth. This refutes the previous possibility that the Earth is located between these asteroids. Logically speaking, if the travel duration is short, it could mean the spacecraft consumes more energy to travel faster. Asteroid 3474 consumes 58 463.0 kg and asteroid 88 consumes 54 897.8 kg. There is not much difference in the fuel consumption that could result in a 1500 days discrepancy. Hence, it is suspected there is a possible external factor affecting the results.

### 5.2.5 Analysis on the Ratio and the Total Fuel Consumption and Total Mission Duration

The lowest minimum total fuel consumption is the trajectory to asteroid 3135 with 19 965.5 kg and the highest minimum total fuel consumption is 61 821.4 kg to reach asteroid 330. Evaluating their total mission duration, the mission to the asteroid 330 needs only 961.6 days, in contrast, the duration to the asteroid 3135 is 2493.6 days. Therefore, it means that a longer mission duration would decrease the fuel consumption.

The ratio of the results is also studied to see how different the outbound trip to the return trip in term of fuel consumption and mission duration. The return trip fuel consumption is 3.552 to almost 30 times more consuming than the outbound trip. This is due to the huge amount of initial mass on the return trip.

An interesting remarks from the ratio of the return trip mission duration to outbound trip mission duration is that some of the ratio are below 1. It means that the return trip from the asteroids is finished faster than the outbound trip. Evaluating their fuel consumption, it is found that the spacecraft consumes nearly 60 000 kg for the return trip from such asteroids. Therefore, the spacecraft consumes a lot of fuel which reduces its mission duration.

## 5.3 Other Factors Affecting the Results

Despite the asteroids orbital elements, there is a possible external factor affecting the optimization which is the optimizer, MATLAB *fmincon*. MATLAB *fmincon* returns a local minimum of a function. The result could be a global minimum, but it is not certain. Figure 5.22 shows the the difference between local and global minimum.

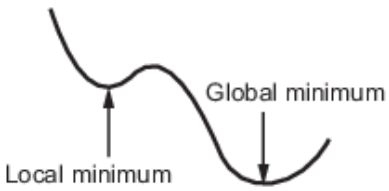


Figure 5.22: The difference between a local minimum and a global minimum. [36]

Local minimum value is smaller than the nearby points, but it might be greater than a point in a distance. Global minimum value is the lowest value that a function can have. This factor explains another possibility that some of the results are not at the global minimum. There are several suggestions on how to achieve a smaller minimum in MATLAB documentation [36]. It mostly explains on how to improve the results by varying the initial guess with statistical method. However, they are outside the scope of the thesis.

## 5.4 First Filter when Choosing Target Asteroids

In the database of synthetic Arjuna-type asteroids, there are more than 4000 asteroids. Each of them has different orbital elements. In this thesis, the asteroids are selected based on the orbital elements so that there are a variety of each element. However, if a person wants to choose an asteroid from the database, it would be better if there are some parameters which can determine which asteroid would potentially have a low fuel consumption.

It is found that the asteroids orbital elements contribute to the fuel consumption and mission duration results as discussed in Section 5.2. After comparing the fuel consumption and the mission duration with the orbital elements, there is no prominent pattern on them except the position of the asteroids with respect to the Earth. However, the vague pattern can be a hint of which values will results in a low fuel consumption. Hence, the orbital elements parameters are chosen based on the discussion in the previous sections. They are shown below.

1. The semi-major axis shall be close to 1 AU.
2. The eccentricity does not show any noteworthy effects.
3. The inclination is as low as possible, preferably below 1°.
4. The position of the asteroid has to be more than 180° away from the Earth (counter clockwise direction) so that the return trip has a closer distance.

# Chapter 6

# Conclusion and Future Work

## 6.1 Conclusion

To conclude the thesis, the optimization is capable of finding trajectories for a round trip mission from LDRO to an Arjuna NEA. Overall, the failure rate of the optimization is 34%. An optimization is considered failed, if there is no convergence found in two days time. The cause of the failure is that the combination of initial guesses that can result in convergence cannot be found during the given time. For the outbound trip, a common set of initial guesses for all asteroids is found and was applied to 29 asteroids with 100% success rate. The important note is that this set of common initial guess is not guaranteed to converge on the first attempt. Some changes are needed for the maneuver duration if the optimization does not result in convergence. The first phase of the return trip has 21% failure rate which is caused by the difficulty to find a combination of initial guesses that can result in convergence. In the following steps of optimization, the failures are caused by the unfavourable orbits from the results of LGA.

The results of the optimizations are intriguing. The lowest minimum fuel consumption in outbound trip is 1166.8 kg and the highest minimum fuel consumption is 4697.5 kg. It is confirmed that the fuel consumption is affected by the orbital elements of the asteroids, especially the position of the spacecraft. In return trip, the highest minimum fuel consumption is 58 463.0 kg which is still in the range of expectation. In contrast, the lowest consumption is beyond expectation with 15 579 kg. The difference of the highest and the lowest fuel consumption is too big if it is affected by the orbital elements alone. MATLAB *fmincon* which is a local minimum solver is suspected as a possible external factor. The solver is highly dependence on the initial guesses. It is possible to achieve a smaller fuel consumption if

the combination of the initial guesses are changed.

## 6.2 Future Work

The project can be continued with the following improvements.

1. Comparing the results of the current optimization method with other optimization method such as those using genetic algorithm.
2. Include spacecraft dimensions so that the solar wind pressure can be considered.
3. Varying the initial guesses for the successful optimizations to ensure a global minimum is achieved.
4. Improving the method of finding a better initial guess.
5. Automating the process of the optimization so that it can change the initial guess by itself if the optimization failed.
6. Automating the entire process of the optimization so that the optimization can continue to the next asteroid when it finds a convergence.
7. More statistical analysis using larger population of asteroids

# Bibliography


[1] Popova, O. P., Jenniskens, P., Emel'yanenko, V., Kartashova, A., Biryukov, E., Khaibrakhmanov, S., ... & Badyukov, D. D. (2013). Chelyabinsk airburst, damage assessment, meteorite recovery, and characterization. Science, 342(6162), 1069-1073.

[2] R. Fork, "Preventing Asteroid Earth Impacts With Laser Technology: Progress and Prospects," in Proceedings of the IEEE, vol. 95, no. 5, pp. 847-848, May 2007. doi: 10.1109/JPROC.2007.893244

[3] NASA. *DART* [Online]. USA: NASA, 2019. [viewed on 22 July 2019]. Available from: https://www.nasa.gov/planetarydefense/dart

[4] NASA. *The Appolo Program* [Online]. USA: NASA, 2009. [viewed on 31 July 2019]. Available from: https://spaceflight.nasa.gov/history/apollo/

[5] M. Gates et al., "NASA's Asteroid Redirect Mission concept development summary," 2015 IEEE Aerospace Conference, Big Sky, MT, 2015, pp. 1-13. doi: 10.1109/AERO.2015.7119163

[6] NASA. *Asteroid Redirect Robotic Mission* [Online]. USA: NASA, 2017. [viewed on 4 August 2019]. Available from: https://www.jpl.nasa.gov/missions/asteroid-redirect-robotic-mission-arrm/

[7] Nelson, M.L., Britt, D.T., Lebofsky, L.A.: Review of Asteroid Compositions. In: Lewis, J.,Matthews, M.S., Guerrieri, M.L. (eds.) Resources of Near Earth Space, Tucson. University of Arizona Press (1993)

[8] Ross, S. D. (2001). Near-earth asteroid mining. Space, 1-24.

[9] TRANS ASTRONAUTICA CORPORATION. *Optical Mining* [Online]. USA: Trans Astronautica Corporation, 2019. [viewed on 22 July 2019]. Available from: https://www.transastracorp.com/optical-mining.html

[10] Calla, P., Fries, D., Welch C.: Asteroid mining with small spacecraft and its economic feasibility. In: Instrumentation and Methods for Astrophysics (astro-ph.IM).

[11] PLANET RESOURCES. *Asteroid mining is the key to our future expansion into space* [Online]. USA: Planet Resources, November 30, 2017. [viewed on 14 June 2019]. Available from: https://www.planetaryresources.com/2017/11/asteroid-mining-is-the-key-to-our-future-expansion-into-space/

[12] Lewicki, C., Diamandis, P., Anderson, E., Voorhees, C., & Mycroft, F. (2013). Planetary resources—The asteroid mining company. New Space, 1(2), 105-108.

[13] Conte, D., Di Carlo, M., Ho, K., Spencer, D. B., & Vasile, M. (2018). Earth-Mars transfers through Moon distant retrograde orbits. Acta Astronautica, 143, 372-379.

[14] NASA. *OSIRIS-REx* [Online]. USA: NASA, 2016. [viewed on 9 June 2019]. Available from: https://nssdc.gsfc.nasa.gov/nmc/spacecraft/display.action?id=2016-055A

[15] NASA. *Hayabusa 2* [Online]. USA: NASA, 2014. [viewed on 9 June 2019]. Available from: https://nssdc.gsfc.nasa.gov/nmc/spacecraft/display.action?id=2014-076A

[16] Fujiwara, A., Kawaguchi, J., Yeomans, D. K., Abe, M., Mukai, T., Okada, T., ... & Barnouin-Jha, O. (2006). The rubble-pile asteroid Itokawa as observed by Hayabusa. Science, 312(5778), 1330-1334.

[17] Landau, D., Dankanich, J., Strange, N., Bellerose, J., Llanos, P., & Tantardini, M. (2013). Trajectories to nab a NEA (near-Earth asteroid).

[18] Bazzocchi, M. C., & Emami, M. R. (2017). Study of arjuna-type asteroids for low-thrust orbital transfer. Journal of Spacecraft and Rockets, 55(1), 37-48.

[19] Capdevila, L., Guzzetti, D., & Howell, K. (2014, January). Various transfer options from Earth into distant retrograde orbits in the vicinity of the Moon. In AAS/AIAA Space Flight Mechanics Meeting (Vol. 118).

[20] Broucke, R. A. (1968). Periodic orbits in the restricted three body problem with earth-moon masses.

[21] Murakami, N., & Yamanaka, K. (2015, March). Trajectory design for rendezvous in lunar Distant Retrograde Orbit. In 2015 IEEE Aerospace Conference (pp. 1-13). IEEE.

[22] Turner, G. (2016). Results of Long-Duration Simulation of Distant Retrograde Orbits. Aerospace, 3(4), 37.

[23] Kohlhase, C. E., & Penzo, P. A. (1977). Voyager mission description. Space science reviews, 21(2), 77-101.

[24] Shirley, D. L. (2003). The mariner 10 mission to venus and mercury. Acta Astronautica, 53(4-10), 375-385.

[25] Guo, Y., & Farquhar, R. W. (2008). New Horizons mission design. Space science reviews, 140(1-4), 49-74.

[26] Strange, N. J., & Longuski, J. M. (2002). Graphical method for gravity-assist trajectory design. Journal of Spacecraft and Rockets, 39(1), 9-16.

[27] Uphoff, C. W. (1989). The art and science of lunar gravity assist. Advances in Astronautical Sciences, 69, 333-346.

[28] Farquhar, R., Muhonen, D., & Church, L. (1984, August). Trajectories and orbital maneuvers for the ISEE-3/ICE comet mission. In Astrodynamics Conference (p. 1976).

[29] Mark Prado. *Space Transportation Lunar Gravity Assist* [Online]. USA: Mark Prado, 2019. [viewed on 13 August 2019]. Available from: https://www.permanent.com/space-transportation-lunar-gravity-assist.html

[30] NASA. *GMAT* [Online]. USA: NASA, 2011. [viewed on 31 July 2019]. Available from: https://software.nasa.gov/software/GSC-16228-1

[31] NASA. *GMAT* [Online]. USA: NASA, 2019. [viewed on 31 July 2019]. Available from: https://sourceforge.net/projects/gmat/

[32] NASA. *SPICE Concept* [Online]. USA: NASA, 2019. [viewed on 9 September 2019]. Available from: https://naif.jpl.nasa.gov/naif/spiceconcept.html

[33] Jedicke, R., Sercel, J., Gillis-Davis, J., Morenz, K. J., & Gertsch, L. (2018). Availability and delta-v requirements for delivering water extracted from near-Earth objects to cis-lunar space. Planetary and Space Science, 159, 28-42.

[34] Muirhead, B. K., & Brophy, J. R. (2014, March). Asteroid redirect robotic mission feasibility study. In 2014 IEEE Aerospace Conference (pp. 1-14). IEEE.

[35] MATLAB. *Constrained Nonlinear Optimization Algorithms* [Online]. USA: MATLAB, 2019. [viewed on 2 August 2019]. Available from: https://se.mathworks.com/help/optim/ug/constrained-nonlinear-optimization-algorithms.html

[36] MATLAB. *Local vs. Global Optima* [Online]. USA: MATLAB, 2019. [viewed on 11 September 2019]. Available from: https://se.mathworks.com/help/optim/ug/local-vs-global-optima.html